Design of Reliable Fluid Power Pitch Systems for Wind Turbines

Liniger, Jesper

DOI (link to publication from Publisher):
10.5278/VBN.PHD.ENG.00040

Publication date:
2018

Document Version
Publisher's PDF, also known as Version of record

DESIGN OF RELIABLE FLUID POWER PITCH SYSTEMS FOR WIND TURBINES

BY
JESPER LINIGER

DISSERTATION SUBMITTED 2018

AALBORG UNIVERSITY
DENMARK

Design of Reliable Fluid Power Pitch Systems for Wind Turbines

Ph.D. Dissertation

Jesper Liniger

Dissertation submitted January, 2018

Dissertation submitted: January, 2018

PhD supervisor: Prof. Henrik C. Pedersen
Aalborg University

Assistant PhD supervisor: Assoc. Prof. Mohsen Soltani
Aalborg University

PhD committee: Associate Professor Zhenyu Yang
Aalborg University

Professor Andrew Plummer
University of Bath

Professor Ronald J. Patton
University of Hull

PhD Series: Faculty of Engineering and Science, Aalborg University

Department: Department of Energy Technology

ISSN (online): 2446-1636
ISBN (online): 978-87-7210-144-6

Published by:
Aalborg University Press
Langagervej 2
DK – 9220 Aalborg Ø
Phone: +45 99407140
aauf@forlag.aau.dk
forlag.aau.dk

Printed in Denmark by Rosendahls, 2018

Abstract

Recent field studies of failures in wind turbines have indicated that pitch systems are the largest contributor to both failures and downtime. The subject of this thesis is, therefore, to reduce failures and downtime of wind turbines through failure analysis of pitch systems including Fault Detection and Diagnosis (FDD) of critical faults.

Most modern Horizontal Axis Wind Turbines (HAWT) employ pitch systems for adjusting the blade pitch angle. Hereby an aerodynamic brake effect is created by appropriate adjustment of the blade pitch angle. Blade angle adjustment is used in both normal operating conditions and in the event of an emergency shutdown for stopping hub rotation. The pitch system, therefore, serves as the primary safety system of wind turbines. Two actuator types exist, using either electrical drives or fluid power cylinder drives. This thesis considers the latter.

A contribution of this thesis is a design tool for pitch systems which enables identification of critical failure modes and root causes in terms of both safety and reliability. The design tool builds on qualitative industry methods and presents a validated systematical framework usable even when very limited information is available on component failures. Amongst others, the design tool results indicate gas leakage in accumulators and valve coil malfunction to be critical faults for conventional pitch systems in terms of safety and reliability respectively. The design tool is further employed in a comparative study of a conventional pitch system concept to a fully hub-contained system. Conclusions are that both an increased safety and reliability is obtained by a hub-contained system supplied by a common unit with a pressurized reservoir.

This thesis furthermore makes two contributions within the area of FDD in fluid power. The first contribution covers the development and application of detection methods for gas leakage of fluid power accumulators. A signal-based method utilizing only the accumulator fluid pressure signal is shown to detect gas leakage for a wide range of operating conditions above rated wind speed. Results are validated experimentally in a multi-fault environment on a test setup allowing for both gas leakage and fluid leakage. A model-based gas

leakage estimation method is validated on the same setup. Results show that detection is permitted when accumulators are initially charged during wind turbine start-up. A combination of the signal and model-based methods, therefore, facilitates detection in a wide range of operating conditions.

The second contribution within FDD covers the development and application of a detection method for the early signs of coil failure in solenoids valves. The early signs of failure are characterized through accelerated lifetime tests. A model-based detection method is validated on a test setup allowing for fault injection in a range of operating conditions, i.e. at changing ambient temperatures and convection conditions. The test results show reliable detection of coil faults before failure.

Synopsis

Nylige feltundersøgelser af fejl i vindmøller har vist, at pitch-systemer forårsager flest fejl og er skyld i størstedelen af vindmøllers nedetid. Hovedformålet i denne afhandling er, at reducere fejl og nedetid i vindmøller gennem fejlanalyse af pitch-systemer, samt fejldetektion og diagnose af kritiske fejl.

I de fleste moderne horisontalakse vindmøller anvendes pitch-systemer til at dreje vingerne omkring deres længdeakse. Når vingerne drejes, skabes en aerodynamisk bremse. Denne bremse bruges både i normal drift og ved nødstop, for at bremse eller stoppe navets rotation. Pitch-systemet fungerer derfor som det primære sikkerhedssystem i vindmøller. Der benyttes enten elektriske motorer eller hydrauliske cylinderdrev til pitch-systemer. Denne afhandling omhandler sidstnævnte type.

Denne afhandling bidrager blandt andet med et designværktøj til pitch-systemer, der gør det muligt, at identificere kritiske fejlmåder og årsager både med hensyn til sikkerhed og pålidelighed. Designværktøjet bygger på kvalitative industrielle fejlanalyse metoder og er brugbart selvom der foreligger meget begrænset information om komponentfejl. Designværktøjet er valideret op mod de seneste feltundersøgelser af fejl i vindmøller. Resultater, forekommet ved anvendelse af designværktøjet, viser at gaslækage i akkumulatorer samt spolefejl i magnetventiler udgør kritiske fejl i forhold til henholdsvis sikkerhed og pålidelighed. Yderligere anvendes designværktøjet til sammenligning af et konventionelt pitch system og et koncept, hvor både forsyning og cylinderdrev monteres i navet. Konklusionen er, at både sikkerhed og pålidelighed øges ved hjælp af et fuldt navmonteret pitch system, hvor cylinderdrevene forsynes af en fælles enhed med tryk-sat tank.

I afhandlingen gøres yderligere to bidrag indenfor fejldetektion og diagnose af hydrauliske systemer. Det første bidrag vedrører udvikling og test af detektionsmetoder til gaslækage i akkumulatorer. En signalbaseret metode, der kun benytter en enkelt olietryksmåling, påvises at kunne detektere gaslækage for en lang række driftsforhold over den nominelle vindhastighed. Metoden valideres eksperimentelt på en testopstilling, der tillader to samtidige fejl i form af både gas- og olielækage. Dermed påvises også robusthed af metoden overfor olielækage. En modelbaseret metode til estimer-

ing af gaslækage valideres ligeledes på testopstillingen. Resultaterne viser, at metoden muliggør estimering af gaslækage, idet akkumulatoren oplades når en vindmølle startes. Tilsammen muliggør den signal og modelbaserede metode derfor detektion af gaslækage i et bredt arbejdsområde.

Det andet bidrag vedrører udvikling og anvendelse af en metode til detektion af de tidlige indikationer af spolefejl i magnetventiler. De tidlige indikationer på spolefejl er karakteriseret ved hjælp af accelererede levetidstest. Detektionsmetoden valideres eksperimentelt på en testopstilling, som muliggør introduktion af fejl ved varierende driftsforhold. Testresultaterne bekræfter, at metoden pålideligt kan alarmere inden forekomsten af spolefejl.

Contents

Preface

This thesis is submitted as a collection of papers in fulfillment of the requirements for the degree of Doctor of Philosophy at the Department of Energy Technology, Aalborg University, Denmark. The work has been carried out at the Department of Energy Technology, Aalborg University Campus Esbjerg, in the period from January 2015 to January 2018 under the supervision of Professor Henrik C. Pedersen and Associate Professor Mohsen Soltani. During the project period, I have been a visiting researcher in the Department of Mechanical Engineering, University of Manitoba, Winnipeg, Canada, from July to September of 2016 under the supervision of Professor Nariman Sepehri. This work has been conducted in cooperation with the industrial partner Hydratech Industries Wind Power under the project "Future Hydraulic Pitch Systems" and is partially supported by Energistyrelsen (EUDP Project No. 64013-0510).

In addition to the enclosed papers, a contribution has also been made to an investigation of using active damping in the pitch controller to lower fatigue loads in wind turbines [76].

I would like to thank all my colleagues at the Department of Energy Technology, Aalborg University and Department of Mechanical Engineering, University of Manitoba, for providing resourceful and positive research environments. I would like to thank my supervisors Professor Henrik C. Pedersen and Associate Professor Mohsen Soltani for many valuable on and off-topic discussions, and I am especially grateful for their ability to create excellent circumstances for both professional and personal development. Also, I would like to thank Professor Nariman Sepehri and his talented team of researchers for contributing to an excellent stay at the University of Manitoba both for me and my family. I appreciate that Daniel B. Rømer, a friend, and former colleague, recommended me to pursue a Ph.D. degree through this project. In addition, I would like to thank Søren Stubkier from Hydratech Industries for providing valuable input from the industry during the project.

Lastly, I would like to express my sincere gratitude to my wife and her endless support, and also to our two sons for always reminding me of the truly important things in life.

Jesper Liniger
Aalborg University, January 29, 2018

Part I

Extended Summary

1 Introduction

1.1 Motivation

Wind turbines are one of the major contributors of renewable energy and an increase in worldwide capacity is expected [24]. The biggest potential for increasing the capacity, especially in Europe and Asia, is the installation of offshore turbines [55]. Currently, however, the Cost Of Energy (COE) from offshore turbines is double compared with onshore turbines. This means a reduced competitiveness relative to other renewable energy sources. The increased COE is both a consequence of high CAPEX and OPEX [55]. The ambition to reduce installation costs has led manufacturers to develop larger and more powerful turbines aimed at the offshore sector [20]. However, the energy loss due to downtime is proportional to the turbine capacity and high availability, therefore, becomes increasingly more important. Availability, being the ratio of potential and actual operating time, is dependent on turbine reliability and maintenance time. Therefore, strategic maintenance aided by condition monitoring and increased reliability is pointed out as main factors in reducing the COE for wind turbines [40, 88].

Through the past decade, several studies on failures in wind turbines have been conducted to reveal reliability and downtime issues in turbine subsystems [15, 37, 71, 81, 93]. The studies emphasize the gearbox as the most critical sub-system for smaller (<1MW) older (prior-2005) turbines. However, for larger (>1.5MW) and newer (post-2005) turbines, the pitch system is indicated as the most critical sub-system. Figure 1.1 shows the overall failure rate distribution from five major sub-systems of the turbine based on two of the most recent studies [15, 93]. Clearly, the pitch system is associated with the highest failure rate. Wilkinson et al. [93] also mention that the pitch system, with over 20%, is the main contributor to downtime of turbines. It is noted, that modern wind turbines employ either electrical and fluid power pitch systems with a 50/50 distribution amongst the entire population [19]. The field failure study by Carroll et al. [15] only considers fluid power pitch systems.

Evidently, improving reliability by design and reducing downtime of pitch

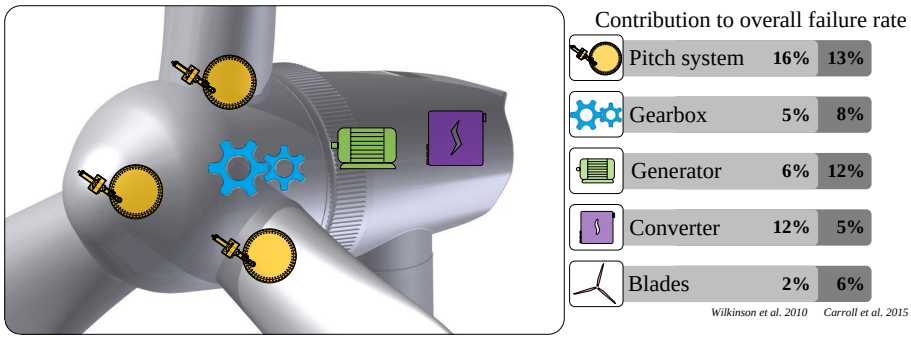

Fig. 1.1: Sub-system failure distribution for wind turbines based on field studies by Wilkinson et. al [93] and Carroll et al. [15]

systems through condition monitoring poses a significant opportunity for lowering the COE produced by modern wind turbines. This thesis takes its offset in fluid power pitch systems which are preferred on modern offshore turbines by two of the major turbine manufacturers MHI Vestas Offshore Wind and Siemens Gamesa Renewable Energy.

1.2 Background

The research disseminated in this thesis is conducted as a part of a development project in cooperation with Hydratech Industries Wind Power and co-funded by the Danish Energy Agency (EUDP Grant number: 64013-0510). Hydratech Industries Wind Power provides fluid power solutions for wind turbines hereunder pitch systems. The aim of the development project is to increase reliability and availability of pitch systems significantly compared to current electrical and fluid power systems.

1.3 Wind Turbine Configuration and Operation

The three-bladed up-wind Horizontal Axis Wind Turbine (HAWT) presents the state-of-the-art configuration for modern multi-megawatt turbines. A conceptual sketch of the HAWT is seen in Figure 1.2. The dimensions are taken from the 5MW reference turbine defined by the National Renewable Energy Laboratory (NREL) [50]. This turbine is the basis for the benchmark turbine simulation model implemented in the Fatigue, Aerodynamics, Structures, and Turbulence software (FAST) [49] which is used throughout this thesis. Further details on the benchmark model are given in section 2.3.

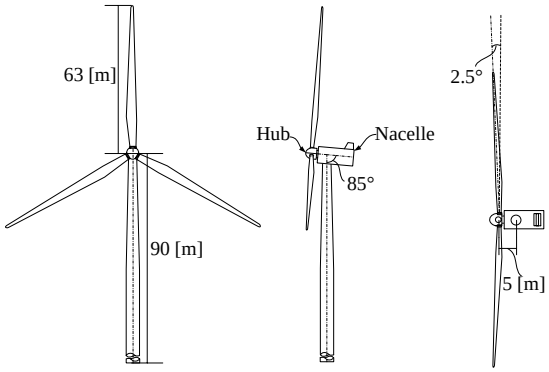

Fig. 1.2: Three-bladed up-wind Horizontal Axis Wind Turbine with dimensions according to the 5MW NREL reference turbine [50]

Modern multi-megawatt turbines are operated according to the variable speed/variable pitch principle. Variable generator speed allows for the turbine to be operated more efficiently than fixed speed turbines at a larger range of wind speeds. The subsequent variable electrical frequency is matched with the grid frequency using a power electronic converter. Variable pitch enables the blades to pitch along the longitudinal axis in order to create an aerodynamic brake which also increases the operating wind speed range. Steady-state variable speed/variable pitch operation is divided into three main wind speed regions as shown in Fig. 1.3.

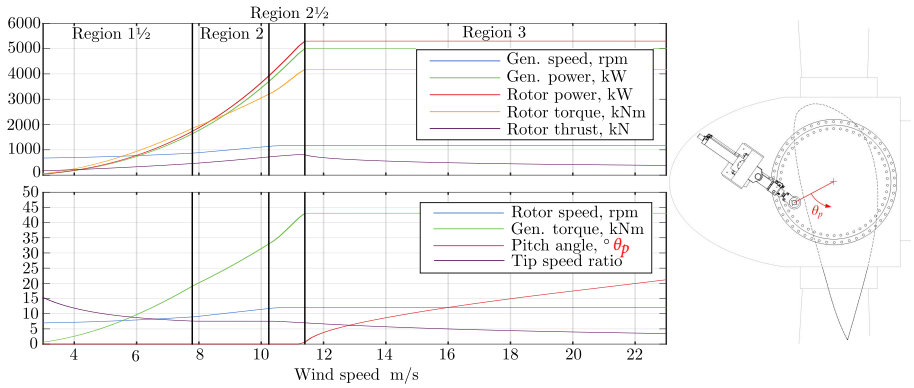

Fig. 1.3: Steady state variable speed/variable pitch operating regions according to the 5MW NREL reference turbine. Based on a figure from the work by Pedersen et al. [76].

In region 1, the wind turbine is prepared for power production where hub rotation is initialized. In region 1½, power production is initiated where the

generator speed and torque are ramped up from the cut-in wind speed at 3m/s. In region 2, the rotor to wind speed ratio, denoted as the tip speed ratio, is maintained at a constant value yielding optimal wind power take out [34]. Fixed tip speed ratio is kept until region 2½ which is a transition from fixed tip speed ratio to fixed rotor speed until the turbine produces rated power at rated wind speed. In this case, 5MW and 11.4m/s respectively. The blade pitch angle reference is kept constant at $\theta_p = 0^\circ$ up until region 3. Constant rated power production is enabled during region 3 by pitching the blades according to the reference given by the red curve in the lower graph of Fig. 1.3. Region 3 remains until cut-off wind speed at 25m/s where power production is terminated and hub rotation is stopped. Pitch systems used not only for adjusting the power take out of the wind, but also in emergency situations by creating an aerodynamic brake to prevent structural damage to the turbine. For fluid power pitch systems, this is obtained by fully extending the pitch cylinders bringing the blades to an angle of $\theta_p = 90^\circ$. Pitch systems are therefore a central part of the emergency shutdown system and must be operable even in the event of a power outage.

1.4 Research Hypothesis

Following the discussions in the previous sections, reliability-based design and condition monitoring of fluid power pitch systems have the potential to significantly reduce the COE produced by wind turbines. It is noted, that condition monitoring is regarded a sub-category of Fault Detection and Diagnosis (FDD).

While aiming for more reliable systems, a potential conflicting design objective exists, because pitch systems are also central to the emergency shut down system of turbines. The safety integrity of the system must therefore not be violated by reliability increasing measures. In order to create more reliable and safe designs, the critical failure modes and root causes of current systems must be identified and mitigated. A review, outlined in chapter 3, reveals that such information is currently only available on a general level and that the failure analysis methods are not sufficient in their formulation to fully cover fluid power pitch systems in terms of reliability and safety. Thus, in relation to improving the safety and reliability by design and including FDD, the research hypothesis follows:

- It is possible to formulate a design framework for fluid power pitch systems which considers both safety and reliability to identify critical failure modes and root causes.
- It is possible to increase safety and reliability of fluid power pitch systems by employing Fault Detection and Diagnosis (FDD) for critical

failure modes and root causes.

1.5 Outline of the Papers

The thesis is constructed as an extended summary based on the contribution of published papers. The extended summary describes the background, motivation for the project and summary of the contributing papers.

The chronology of the papers follows Fig. 1.4 and the papers are described as follows:

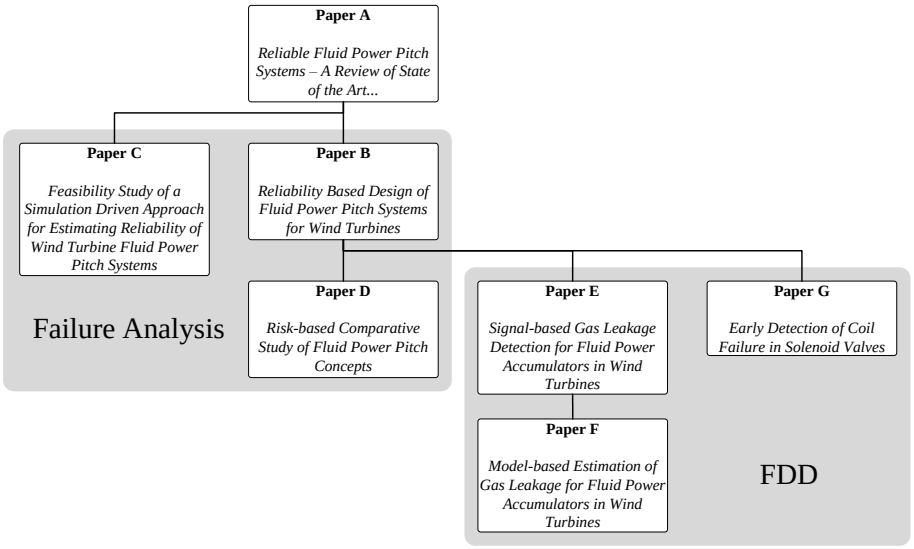

Fig. 1.4: Chronology of published papers constructing the basis for this thesis.

Paper A [56]

The aim of this paper is to present a brief state-of-the-art review of the areas related to reliability within fluid power; Failure analysis, FDD and Fault-Tolerant Control (FTC). Also, the paper gives an overview of fluid power pitch concepts available in patents and patent applications. Paper A presents a starting point for the subsequent work in this thesis.

Paper B [61]

The review in paper A showed that the qualitative basis for performing reliability evaluation of fluid power pitch systems was insufficient. Thus, paper B presents a design tool based on Fault Tree Analysis (FTA)

and Failure Mode and Effects Criticality Analysis (FMECA) for performing qualitative failure analysis. The design tool takes both reliability and safety into account by the use of the Risk Priority Number (RPN). Feasibility of the design tool is shown in a case study of a pitch system where results are correlated to field failure data. Among others, the results highlight a significant risk reduction when monitoring accumulator leakage, which subsequently has lead to the work in papers E and F.

Paper C [59]

The field failure rates available do not provide sufficient detail for performing reliability evaluation and mitigating failures in current pitch system concepts. While paper B presented a qualitative approach, this paper aims to quantitatively estimate failure rates by utilizing conditions from a simulation model of a pitch system operating in a wind turbine. The simulation model is obtained from the methods presented in paper D. Results show a significant discrepancy between estimated and field failure rates presumably caused by an out-dated estimation procedure for fluid power components.

Paper D [58]

Based on the pitch concepts reviewed in paper A and the design tool developed in paper B, this paper presents a comparative study of two pitch concepts. The two concepts are a conventional system design and a distributed system design. Conventional systems share a common supply and actuation circuits in the nacelle and hub respectively. Distributed systems are fully contained in the hub with individual supply units. The main results indicate that the two concepts are equally safe, while the conventional system is the most reliable. The paper was nominated for "Best Paper" by the Global Fluid Power Society.

Paper E [60]

Following the conclusion from paper B, this paper presents the development and application of a signal-based gas leakage detection method for accumulators in wind turbines. The method depends only on an accumulator fluid pressure signal processed using Multi Signal Decomposition (MSD) based on wavelets. The efficacy of the method is proven on an experimental setup and simulations are used for validation in a further operating range. The results show that the method is indeed working, however, limitations exist for lower ambient temperatures.

Paper F [57]

This paper attempts to increase the usable operating range for accumulator gas leakage detection by application of an Extended Kalman Filter

(EKF). The model-based scheme uses sensors already available on most fluid power pitch systems such as ambient temperature, accumulator pressure, and pitch cylinder position. Experimental results show that the method is not precise under normal turbine operating conditions. However, precise results are obtained when the accumulators are initially charged as the turbine starts up.

Paper G [62]

The failure analysis presented in paper B can be used to show that coil failure in solenoid valves present a significant reliability issue of pitch systems. This paper addresses coil failure both by experimentally investigating coil failure characteristics and also by application of a detection method. The failure characteristic shows that early signs of coil failure are present in the coil current signal before burn-out. A detection method is developed for detecting these early signs of coil failure based on the EKF. The method proves to reliably detect the early signs of coil failure on an experimental setup in the event of changing ambient temperature, convection, and fluid flow conditions.

2 Pitch System Description

2.1 System Layout

A conventional type fluid power pitch system is shown in Fig. 2.1. Component label descriptions are given in Table 2.1. While turbine specific pitch system diagrams remain confidential, the presented layout is based on knowledge of such actual systems. Conventional systems consist of three fluid power cylinder drives, each connected to the blade root in the hub and a common open circuit Hydraulic Power Unit (HPU) located in the nacelle. The cylinder drives and HPU are connected by a rotary union R1.

The purpose of the pitch system is to perform two main functions; closed-loop pitch angle control(normal operation) and emergency shutdown. Also, a braking cylinder C2 is normally employed for locking blade pitch rotation when the turbine is stopped. Closed-loop pitch angle control is conducted by proportional valve V6 supplying differential cylinder C1 which is fitted with position feedback. Regenerative flow is used when cylinder C1 extends in order to both lower flow consumption under normal operation and also reduce accumulator size needs when performing an emergency shutdown. Either configuration 1 or 2 are used as energy storage for emergency shutdown. In configuration 1 (blue) the pressurized accumulator A1 is blocked from the main circuit in normal operation by valve V5 and valve V8 opened when an emergency shutdown is needed. Accumulator A2 is used in configuration 2 (red) both as emergency storage and as a supplier of surplus flow during high pitch activity. Accumulator A3 is not used in configuration 2.

The supply circuit located in the nacelle consists of a fixed-speed fixed-displacement pump where the excess flow is directed through valve V2 to the reservoir. Fluid is cleaned through the low-pressure return filter F1 which is fitted with a clogging indicator.

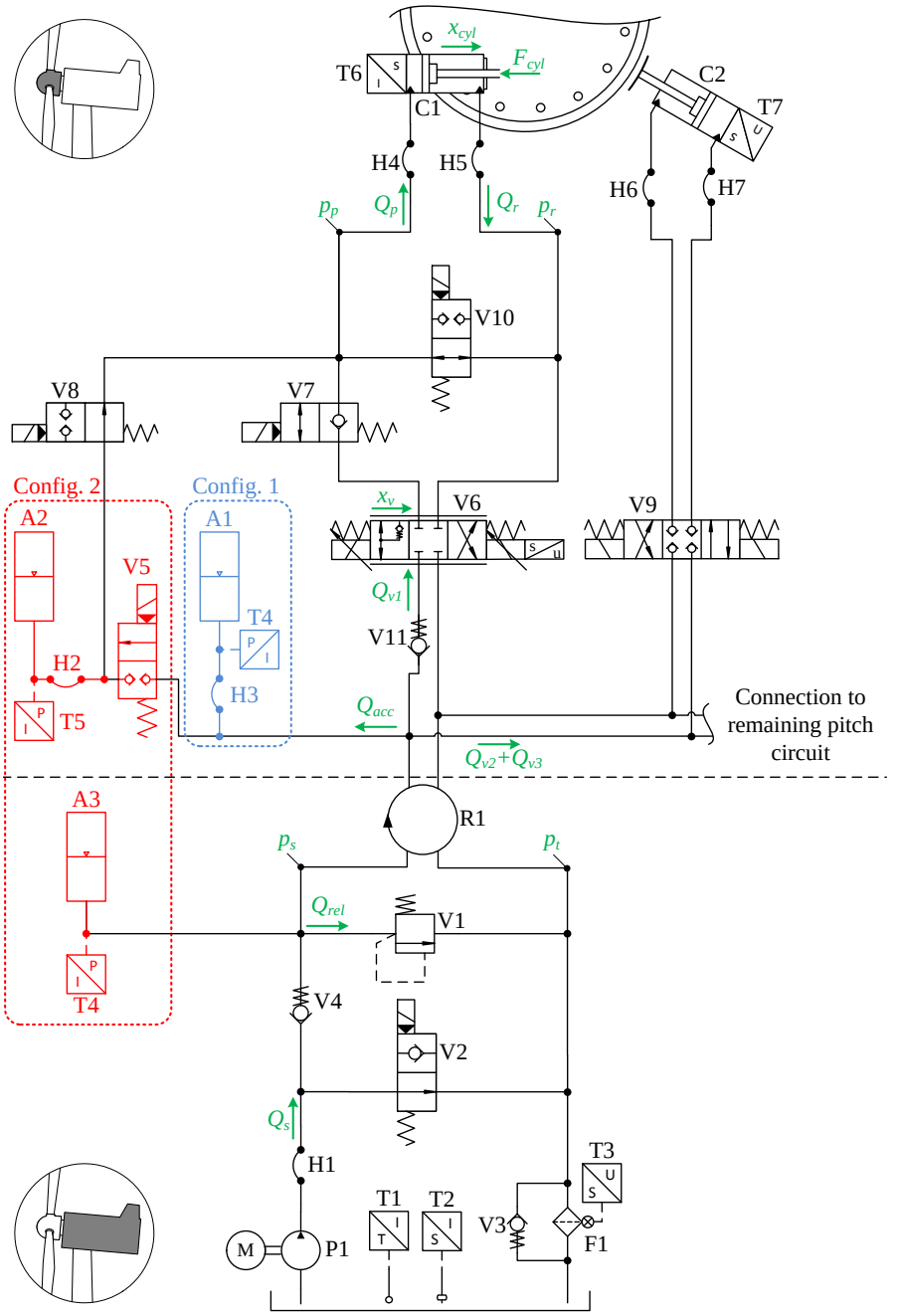

Fig. 2.1: Conventional type fluid power pitch system diagram. All valves are shown in the de-energized state. Sign conventions and model notations are given in green. Based on figures from paper B and paper F.

Table 2.1: Description of component labels. Based on Table from paper F.

Label	Description
V1	Pressure relief valve
V2,V5,V7,V8,V10	Two way solenoid valves
V3,V4	Check valves
V6	Proportional solenoid valve
V9	Three way solenoid valve
C1	Differential pitch cylinder
C2	Differential locking cylinder
H1-H7	Flexible hoses
A1,A2	Gas charged piston accumulators for emergency shutdown
A3	Gas charged piston accumulator for supply
P1	Fixed-speed fixed-displacement gear pump
F1	Return line filter with clogging indicator
T1	Reservoir fluid temperature sensor
T2	Reservoir fluid level sensor
T3	Filter clog sensor
T4	Accumulator pressure sensor
T5	Emergency accumulator pressure sensor
T6	Pitch piston position sensor
T7	Locking piston position sensor

Note that the pitch system shown in Fig. 2.1 does not consider a fluid cooling circuit which is often used to limit the fluid temperature. Failure related to the cooling circuit is therefore not accounted for in the further analysis. Also, it is not uncommon for actual systems to employ multiple cylinders and accumulators. For simplicity, only a single pitch cylinder C1 and single emergency accumulator A1 or A2 are depicted in Fig. 2.1.

2.2 Operational Modes

Pitch system operational modes are normally divided into the following four modes [61]. These are important both to give a basic understanding of pitch systems and also because the operational modes are used in the failure analysis for systematically evaluating the severity of faults. Further details are given in chapter 3.

Start-up is a procedure for initializing the pitch system for region 1 operation as described in section 1.3. Firstly, all transducer values are checked not to be out-of-bounds and all valves are in their de-energized state. The emergency accumulators A1 or A2 are pressurized by switching the pump on and energizing V2 until the pressure read by T5 or T4 reaches the desired level. Afterwards, the locking cylinder is retracted using valve V9 and pitch cylinder C1 retracts to $\theta_p = 0^\circ$.

Power regulation also referred to as normal operation, cover regions $1^1/_2$ to 3. As previously mentioned, the pitch cylinder is controlled in closed-loop using proportional valve V6 according to the pitch angle reference seen in Fig. 1.3. Valves V7 to V8 are energized. Valve V2 is switched on or off when the supply pressure read by sensor T4 is below or above the threshold limits respectively.

Normal shutdown is initiated either when the wind speed falls sufficiently below cut-in in region 1 or when the turbine is brought to a scheduled stop. The pitch angle reference is set to $\theta_p = 90^\circ$. The locking cylinder C2 is engaged when the pitch cylinder C1 is fully extended. Lastly, the supply circuit is de-energized.

Emergency shutdown is performed in the event of a severe failure to the turbine. All valves and the pump are de-energizing whereby accumulator A1 or A2 releases flow through valve V8 to permit regenerative extending of the pitch cylinder C1.

2.3 Simulation Model

Simulated operational data are used throughout this thesis for benchmarking both failure rate models and fault detection methods. Simulations are used because of limited access to a testing turbine and also to reduce testing time. Where appropriate, the methods developed in this thesis are further validated by laboratory experiments emulating real turbine operation.

The simulation model consists of both the fluid power pitch system and the 5MW NREL benchmark turbine implemented in FAST. The fluid power pitch system is modeled in MATLAB© Simulink© and co-simulated with

FAST. A brief introduction of the model is given here. This is developed by Pedersen et al. [76] including the accumulator model presented in paper E. The mentioned papers can be consulted for system dimensions and constants which are not replicated here.

The pitch system is modeled in normal operation and the locking circuit is omitted, i.e. disregarding components C2 and V9. Figure 2.1 shows relevant model notations and sign conventions used throughout this thesis.

Actuation circuit

The actuation circuit covers the pitch cylinder C1 and proportional valve V6. Pressure drop across valves V7 and V11 is neglected. The actuation circuits are named $i : \{1, 2, 3\}$. The pressure build-up in the piston and rod side chambers of the pitch cylinder are described by the continuity equations respectively:

$$\dot{p}_{p,i} = \frac{\beta_{e,p,i}}{V_p(x_{cyl,i})} \left(Q_{p,i} - A_p \dot{x}_{cyl,i} \right) \tag{2.1}$$

$$\dot{p}_{r,i} = \frac{\beta_{e,r,i}}{V_r(x_{cyl,i})} \left(Q_{r,i} - A_r \dot{x}_{cyl,i} \right) \tag{2.2}$$

$V_{p,i}$ and $V_{r,i}$ are piston and rod side volumes including hose volumes and are dependent on the piston position $x_{cyl,i}$. $Q_{p,i}$ and $Q_{r,i}$ are piston and rod side cylinder flows defined in Fig. 2.1. $A_{p,i}$ and $A_{r,i}$ are piston and rod areas respectively. $\beta_{e,p,i}$ is the effective bulk modulus of the oil in the piston chamber control volume as given in:

$$\beta_{e,p,i} = \frac{1}{\frac{1}{\beta_{oil}} + \frac{V_{\%air,i}}{V_{p,i}\beta_{air,i}}} \tag{2.3}$$

where the volume content of air for the piston chamber being determined as $V_{\%air,i} = \left(p_0 \, {V_{\%air,0}}^{\kappa} / p_{p,i} \right)^{\frac{1}{\kappa}}$. $\kappa = 1.4$ and $\beta_{air,i} = 1.4 p_{p,i}$ holds by assuming an adiabatic process. The reference p_0 is selected to atmospheric pressure and $V_{\%air,0}$ is determined accordingly. Similar assumptions hold for $\beta_{e,r,i}$.

The flows across proportional valve V6 are modeled in equations (2.4)-(2.5). Flow across the check valve is assumed laminar while all other flows are modeled by the orifice equation assuming fully developed turbulent flow

[68].

$$Q_{p,i} = \begin{cases} K_v(x_{v,i})\sqrt{|p_s - p_{p,i}|}\text{sign}(p_s - p_{p,i}) & , \quad x_{v,i} \geq 0 \\ -K_v(x_{v,i})\sqrt{|p_{p,i} - p_t|}\text{sign}(p_{p,i} - p_t) & , \quad x_{v,i} < 0 \end{cases} \tag{2.4}$$

$$Q_{r,i} = \begin{cases} K_{cv}(p_{r,i} - p_s - p_{cv,c}) & , \quad x_{v,i} \geq 0 \bigwedge p_{r,i} > p_s - p_{cv,c} \\ 0 & , \quad x_{v,i} \geq 0 \bigwedge p_{r,i} \leq p_s - p_{cv,c} \\ -\phi K_v(x_{v,i})\sqrt{|p_s - p_{r,i}|}\text{sign}(p_s - p_{r,i}) & , \quad x_{v,i} < 0 \end{cases} \tag{2.5}$$

K_v denotes the valve flow coefficient as a function of spool position $x_{v,i}$. p_s and p_t are supply and reservoir pressures respectively. Valve V6 opening areas are matched to the area ratio of the cylinder given by $\phi = {}^{A_r}/_{A_p}$. The check valve is associated with the flow constant K_{cv} and crack pressure $p_{cv,c}$. The valve dynamics are described by a cascade of first and second order systems as given in (2.6) and a slew rate limit of $\dot{x}_{v,max}$. This model structure is found to best describe the input step responses found from the valve data sheet.

$$\frac{x_{v,i}}{u_{v,i}} = \frac{\omega_n^2}{(s^2 + 2\zeta_v\omega_n s + \omega_n^2)(\tau_v s + 1)} \tag{2.6}$$

where $u_{v,i}$ is the input spool reference, ω_n is the natural frequency of the valve, and ζ_v is the damping ratio. τ_v denotes the time constant of the first order system in cascade with the second order dynamics.

The cylinder force in Eq. (2.7) depends on the chamber pressures and a friction force function F_{fric}.

$$F_{cyl,i} = p_{p,i}A_p - p_{r,i}A_r - F_{fric,i}(\dot{x}_{cyl,i}) \tag{2.7}$$

The friction function $F_{fric,i}(\dot{x}_{cyl,i})$ consists of a piston velocity proportional damping force and the Coulomb force.

Supply circuit

The supply circuit consists of the pump P1, relief valve V1 and accumulator A3. The pressure drop across check valve V4 is neglected. The function of the dump valve V2 is to control pump flow Q_s in order to keep supply pressure p_s within a lower $p_{s,low}$ and higher $p_{s,high}$ threshold. This is conducted by a simple hysteresis type controller as given in:

$$Q_s = \begin{cases} Q_{s,nom} & , \quad s_p = 1 \\ 0 & , \quad s_p = 0 \end{cases} \tag{2.8}$$

where s_p is a logic value indicating the state of the pump and $Q_{s,nom}$ denotes the nominal flow from the fixed-speed fixed-displacement pump.

The continuity equation for the accumulator (A1 or A3) follows:

$$\dot{V}_g = -Q_{acc} = -Q_s + Q_{rel} + \sum_{i=1}^{3} Q_{v,i} \tag{2.9}$$

where $\dot{V}_g$ denotes the rate of change for the gas volume contained in the piston accumulator. $Q_{v,i}$ is the valve flow according Fig. 2.1. The oil stiffness is neglected as it is much higher than the gas stiffness. Piston friction is also neglected which leads to equal accumulator gas and fluid pressure. The relief valve flow Q_{rel} is given in Eq. (2.10) where K_{rl} denotes the flow coefficient and $p_{cr,r}$ the crack pressure.

$$Q_{rel} = \begin{cases} K_{rl}(p_s - p_{cr,r}) & , \quad p_s > p_{cr,r} \\ 0 & , \quad p_s \leq p_{cr,r} \end{cases} \tag{2.10}$$

The Benedict–Webb–Rubin (BWR) equation of state is used for describing the relation between the pressure p_s, volume V_g and temperature T_g of a gas with mass m_g which has been found to perform well for fluid power accumulators [33, 74]. The BWR equation of state is given in Equation (2.11).

$$p_s = \frac{RT_g}{\frac{V_g}{m_g}} + \frac{B_0 RT_g - A_0 - \frac{C_0}{{T_g}^2}}{\left(\frac{V_g}{m_g}\right)^2} + \frac{bRT_g - a}{\left(\frac{V_g}{m_g}\right)^3} + \frac{a\alpha}{\left(\frac{V_g}{m_g}\right)^6} + \frac{c\left(1 + \frac{\gamma}{\left(\frac{V_g}{m_g}\right)^2}\right) e^{-\frac{\gamma}{\left(\frac{V_g}{m_g}\right)^2}}}{\left(\frac{V_g}{m_g}\right)^3 {T_g}^2} \tag{2.11}$$

Nitrogen is normally used in gas charged accumulators and the properties are described by the set of empirical constants $\{A_0, B_0, C_0, a, b, c, \alpha, \gamma, R\}$ as found in [29].

The thermal behavior of gas contained in steel type piston accumulators have previously been shown to be well approximated by [33, 74, 80, 83]:

$$\dot{T}_g = \frac{T_a - T_g}{\tau_g} - \frac{T_g}{c_v}\frac{\partial p_s}{\partial T_g}\frac{\dot{V}_g}{m_g} \tag{2.12}$$

$$\tau_g \approx 0.3 \cdot 10^{-5} \cdot p_{pc}\, {V_{acc}}^{0.33} + 86.2 \cdot {V_{acc}}^{0.49} \tag{2.13}$$

where T_a is the ambient temperature and c_v is the specific heat capacity at constant volume. The thermal time constant τ_g depends on the gas precharge pressure p_{pc} and gas volume V_{acc} when the accumulator holds no fluid.

Mechanical coupling

The mechanical coupling describes the linkage between the pitch cylinder and blade bearing. A rigid multi-body model is developed based on Lagrangian mechanics and the Fig. 2.2 shows the notation used.

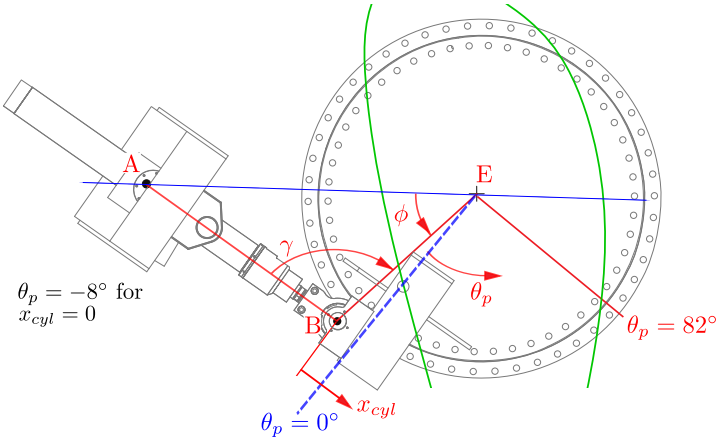

Fig. 2.2: Mechanical coupling between pitch cylinder and bearing including model notation. Figure from the work by Pedersen et al. [76].

Neglecting potential energy changes in the system and using the Lagrange equations yields the system dynamics:

$$J_{eq}\ddot{\theta}_{p,i} - \frac{\partial x_{cyl,i}}{\partial \theta_{p,i}} \frac{\partial^2 x_{cyl,i}}{\partial {\theta_{p,i}}^2} \dot{\theta}_{p,i} = F_{cyl,i} L_{BE} \sin(\gamma_i) + M_{aero,i} \tag{2.14}$$

where the equivalent inertia $J_{eq,i}$ is given by:

$$J_{eq,i} = \left(\left(\frac{\partial x_{cyl,i}}{\partial \theta_{p,i}} \right)^2 m_{pis} + J_b \right) \tag{2.15}$$

L_{BE} is the length between point B and E. The piston mass is given by m_{pis} and J_b denotes the blade inertia. The blade inertia is assumed to be constant and the increase due to deflection is disregarded. The wind flow past the blade generates an aerodynamic torque along the pitch axis and is denoted by $M_{aero,i}$. $M_{aero,i}$ is an output from FAST.

FAST

The NREL 5MW benchmark turbine implementation in FAST is chosen as it presents an open source wind turbine simulation environment offering a suitable compromise between simulation speed and precision needed in this research [49, 50]. FAST considers the flexibility and multi-body dynamics of the major components such as the tower, blades and main shaft. The aerodynamics essentially describing the power conversion from the wind, is

based on the Blade Element Momentum-method (BEM). The software utilizes a three-dimensional flow field considering, amongst others, the wind velocity profile, turbulence intensity and mean wind speed at hub height. The flow field is generated using TurbSim [48] and follows the wind turbine design standard IEC61400-1 Design Load Case 1.2 (DLC) [43]. DLC 1.2 is used for evaluating fatigue loads during normal operation of turbines and in compliance with the standard, three levels of turbulence intensities are considered, high (A,16%), medium (B,14%) and low (C,12%). Turbulence intensities are modeled by the Normal Turbulence Model (NTM). The connection of FAST with the pitch system simulation model is described in the next section.

Model Overview

Figure 2.3 shows a block diagram depicting the simulation model of the pitch system connected to FAST. The outer power control loop determines a collective pitch reference based on the mean wind speed and the generator speed based on Fig. 1.3. The inner pitch angle control loop sets the valve input to the pitch system. The pitch angle is input to FAST. The outputs used from FAST are the aerodynamic torque along each pitch axis and the generator speed. Note that, numerical integrations of pressure gradients and angular pitch acceleration is not depicted in Fig. 2.3.

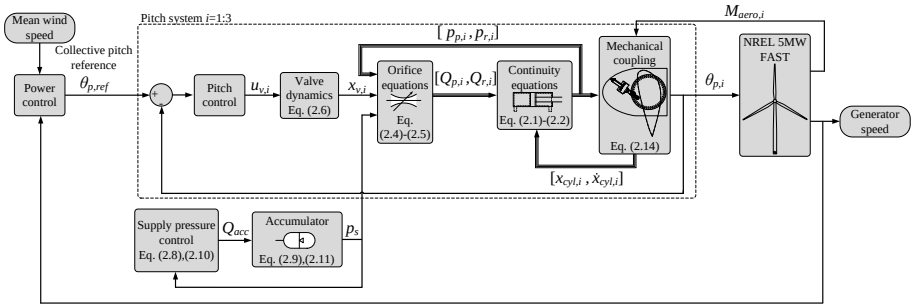

Fig. 2.3: Block diagram of pitch systems simulation model connected to FAST. The diagram depicts one out of three pitch systems.

The simulation model is used further in this thesis both for reliability evaluation and benchmark of fault detection methods.

3 Failure Analysis

A failure analysis identifies the fault mechanisms of a system and how these propagate to reveal critical faults. This helps to make it obvious to the designer which to mitigate or monitor in order to increase safety and/or reliability. A distinction is made between fault and failure, where a fault describes an underlying event leading to the failure of a system [10]. Failure analysis is often performed first qualitatively followed by a quantitative analysis. It is noted that the definition of failure analysis used in paper A and paper B covers only the qualitative part. Generally and in this thesis, it is more convenient to use a definition that covers both the quantitative and qualitative part together.

The chapter is initiated by a description of field data on pitch system failures. This is followed by two sections covering qualitative and quantitative failure analysis respectively.

3.1 Field Failure Data

To give an overview, the used definition for reliability considers a system to be either in a functional or non-functional state. Reliability, $R(t)$, is the probability of a system being in the functional state during its intended life time. The failure rate, $\lambda(t)$, is defined as failure pr. time unit. The failure rate may in special cases be regarded as constant $\lambda(t) = \lambda$, which yields the following relation to reliability [8]:

$$R(t) = e^{-\lambda t} \tag{3.1}$$

For most mechanical systems a constant failure rate assumption is usually not sufficient and the "bathtub curve" is normally more descriptive [8, 9]. As seen in Fig. 3.1, the failure rate progress for fluid power pitch systems follows the bathtub curve for the first six years. A slight infant mortality is seen for the first two years, whereafter the wear out phase continues to year six. The failure rate decreases for years seven and eight. The reasoning behind this phenomenon is not evident from the field data study by Carroll et al. [15].

However, such drop in failure rate may result from extensive services and inspections conducted around year six.

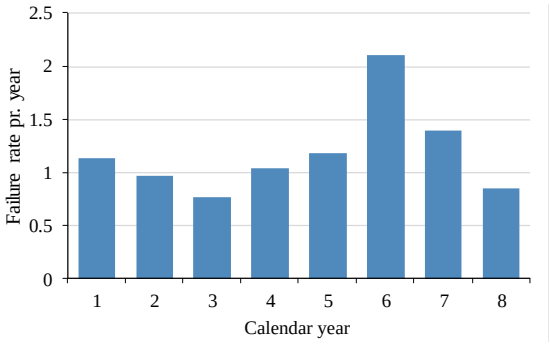

Fig. 3.1: Fluid power pitch system failure rate pr. calendar year. Reproduced from the field data study by Carroll et al. [15].

The fault distribution, similarly from the study by Carroll et al. [15], is shown in Fig. 3.2.

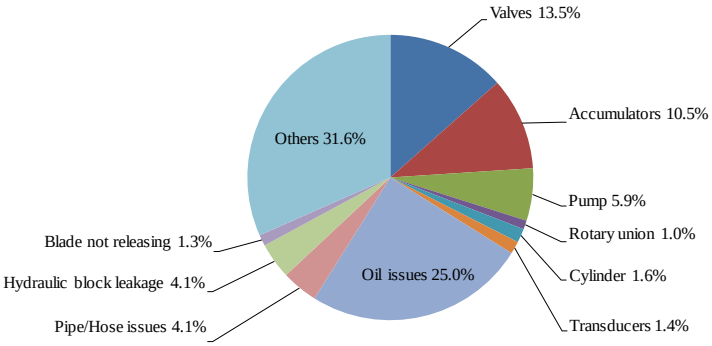

Fig. 3.2: Fault distribution for fluid power pitch systems. Reproduced from the field data study by Carroll et al. [15].

The majority of faults are seen to be related to oil issues. Oil issues cover faults due to low fluid quality and various types of leakage. After this, valves, accumulators, and pumps are top three component contributors to faults. The Others-category consists mainly of unspecified faults in the pitch system.

The presented field data present both failure rate and distribution among major component groups. However, no indication is given to the severity of faults or root causes. Both of which are important for identifying weak spots in current systems and mitigating faults in future designs. The remainder of

this chapter aims to investigate these areas further.

3.2 Qualitative Analysis

The objective of qualitative failure analysis is to identify fault mechanisms and fault propagation, and subsequently to consider the criticality of the fault mechanisms. The qualitative approach is very useful in the case where information on failure rates and reliability for components is very limited. Like for pitch systems, this is also the case for fluid power systems in general [22, 56].

State of the Art

In industry, Fault Tree Analysis (FTA) and Failure Modes and Effect Criticality Analysis (FMECA) are often used for performing qualitative failure analysis [8, 9, 86]. The major drawback of these methods is that they are defined in a very broad sense to cover both software, mechanical, electrical, and hybrid systems [65, 91]. This leads to the results being highly subjective and sensitive to bias. In addition, the time scale of the analysis often exceeds the design process which challenges their use as an actual design tool [12]. Reviews of qualitative methods, see paper A and paper B, reveal two categories in relation to automatic fault propagation analysis in fluid power systems. Automated fault propagation has been considered to make the process more efficient. One category describes automatic fault propagation analysis based on expert knowledge on component failure modes and a circuit diagram [3, 38, 39, 66, 95]. The other category covers methods that likewise automatically solves the fault propagation, but here the component failure modes are based on steady-state simulations models [13, 22, 87]. The methods described in both categories rely on rather extensive software implementations. None of these softwares seemed to have found widespread use and it is considered inefficient to implement the methods for performing analysis of only a pitch system. The approach sought in this work is therefore manual. However, the strict formulation of the presented method certainly makes it viable for software implementation.

Only two of the automatic fault propagation methods were found to also consider the criticality of faults in terms of a risk parameter [22, 87]. Gjerstad et al. determine risk as a product of fault severity and quantitative probability [22] and Stecki et al. [87] augments automatic fault propagation with the Risk Priority Number (RPN). The methods are, however, not usable in a straightforward manner because qualitative failure information is limited and the reasoning for setting the RPN is not described. The design tool presented in the next section addresses these deficiencies by incorporating

industry standard failure analysis methods in the context of wind turbines and fluid power pitch systems into a systematic framework

Design Tool

The design tool developed in paper B is presented in this section. The method is summarized in Fig. 3.3.

The FTA is a top-down approach that allows for analysis of the major top events such as pitch systems failure and propagating to component faults through a fault tree. Thus, the FTA is suitable for identifying the important component faults (failure modes) which can subsequently be used in the Failure Mode and Effects Criticality Analysis (FMECA). For the FTA to be efficient, the system and level of detail are initially defined. The system definition depends on the circuit diagram as given in Fig. 2.1 and a description of operational modes (modes) as given in section 2.2. The level of detail is set through lists of considered failure modes and root causes as given by expert knowledge based on the work by Hunt [42], Watton [92] and Totten [90]. Also, the extent of the analysis is limited through the assumptions of no simultaneous fault events and an initially fault-free system. The fault tree is developed by subdividing each mode into phases. As an example, a phase under the power regulations mode is *cylinder C1 retracting to setpoint*. A phase sets all components in a given state such that the active flow path from supply to the actuator is evident. Generally, all the components connected to the active flow path, which can cause the phase to fail, is then associated with the fault tree under the given phase. Further detail is given in paper B on how the fault tree is developed.

The FMECA is a bottom-up approach used here both to connect failure modes to root causes and introduce the RPN for evaluating risk. At this level, the bottom-up is preferable to achieve the desired level of detail without causing work-overload since only the important failure modes are considered as a result of the FTA. The RPN determining risk can according to Tavner et al. [89] be given as:

$$\mathrm{RPN} = 2^{\mathrm{Severity} + \mathrm{Occurrence} + \mathrm{Detection}} \tag{3.2}$$

and is determined for each failure mode and root cause combination. The RPN depends on three scores, namely *severity*, *occurence* and *detection*. Table 3.1 shows the criteria for setting the scores according to Arabian et al. who considered the RPN in terms of wind turbine taxonomy [2]. The severity score is directly related to the affected operational mode for a given failure mode. For instance, a failure mode causing an emergency shutdown fault in more than one pitch system is rated as catastrophic due to a 2-out-of-3 (2oo3) safety requirement. The 2oo3 safety requirement is used based on the recommendations given in the IEC61400-1 design standard [43] and in the

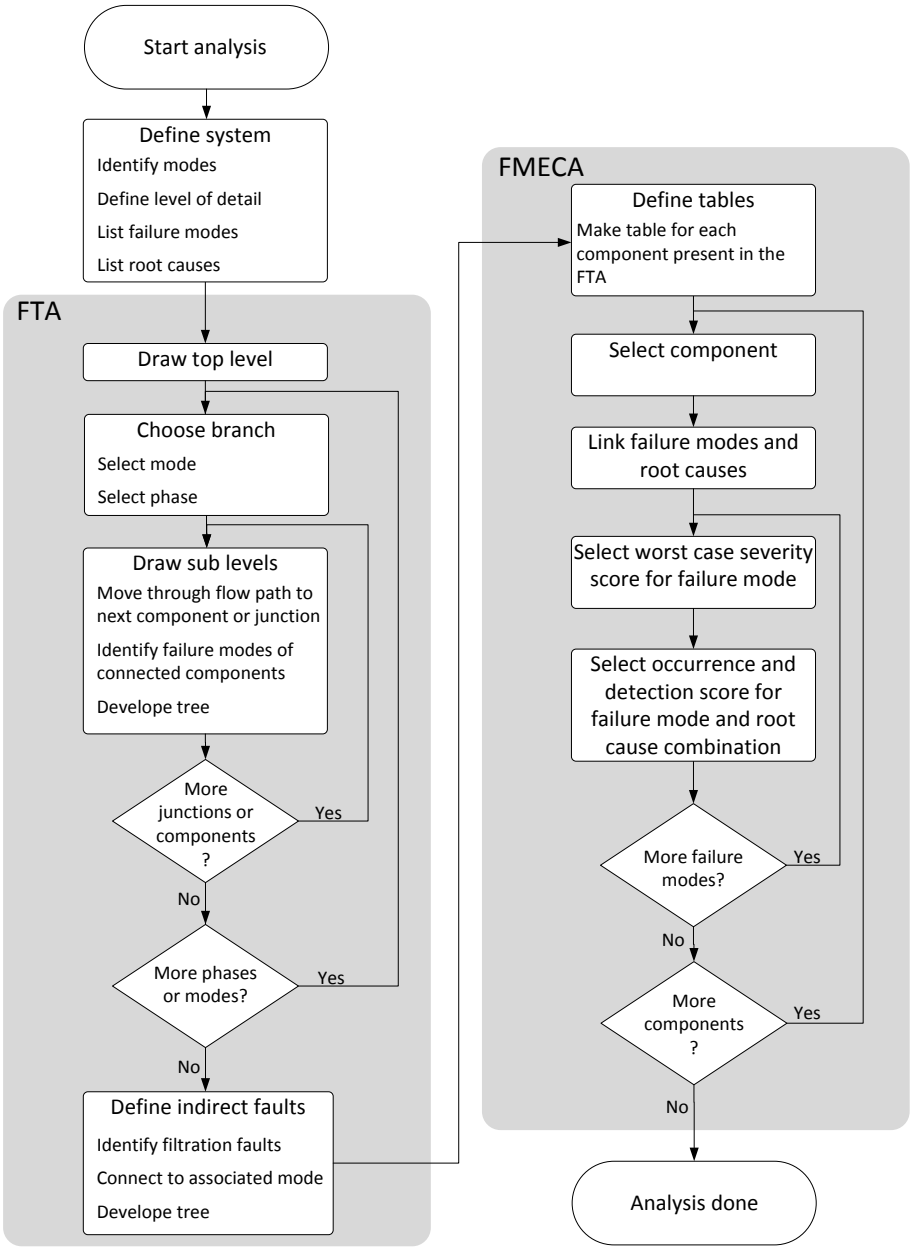

Fig. 3.3: Flow chart describing the design tool used for failure analysis of fluid power systems. Based on figure from paper B.

GL offshore certification guidelines [23]. The occurrence score describes the probability of a given failure mode and root cause combination. The score is difficult to set without knowledge of the actual fault probability. However, results showing good overall correlation to field data are obtained if the score is set relatively between the failure modes based on expert knowledge [61, Fig. 9]. The detection describes the efficiency of monitoring methods applied to the system, thus allowing for analyzing the impact of condition monitoring of failure modes. Further reasoning for setting the scores is evident from the descriptions in paper B.

Table 3.1: Scales for severity, occurrence, and detection reproduced from the work by Arabian et al. [2]. Table from paper B.

Scale	Description	Criteria
	Severity	
1	Category IV (minor)	Electricity can be generated but urgent repair is required
2	Category III (marginal)	Reduction in ability to generate electricity
3	Category II (critical)	Loss of ability to generate electricity
4	Category I (catastrophic)	Permanent structural damage to the turbine
	Occurrence	
1	Level E (extremely unlikely)	Single failure mode probability of occurrence < 0.001
2	Level D (remote)	Single failure mode probability of occurrence is > 0.001 but < 0.01
3	Level C (occasional)	Single failure mode probability of occurrence > 0.01 but < 0.10
5	Level A (frequent)	Single failure mode probability > 0.10
	Detection	
1	Almost certain	Monitoring methods almost always will detect the failure
4	High	Good likelihood that monitoring methods will detect the failure
7	Low	Low likelihood of monitoring methods to detect the failure
10	Almost impossible	No known monitoring method is available to detect the failure

When introducing the RPN it is important to distinguish between risk and reliability. As defined here, the risk is a qualitative measure of the safety integrity, and occurrence is a qualitative measure of reliability.

Results

The results of applying the design tool to the pitch systems presented in Fig. 2.1 (assuming accumulator configuration 2) is presented in Fig. 3.4 and Fig. 3.5.

The failure mode Pareto chart in Fig. 3.4 (a) expectedly reveals that various forms of leakage and valve seizure introduce high risk to pitch systems. Remark that the method distinguished between leakage and rupture. Rupture describes high leakage flow preventing a function to operate. Also evident is that gas leakage from the accumulators is associated with a significant risk. Similar tendencies are also seen for the occurrence of failure modes in Fig. 3.4 (b) though with the addition of electrical related root causes for wire malfunction and controller output malfunction.

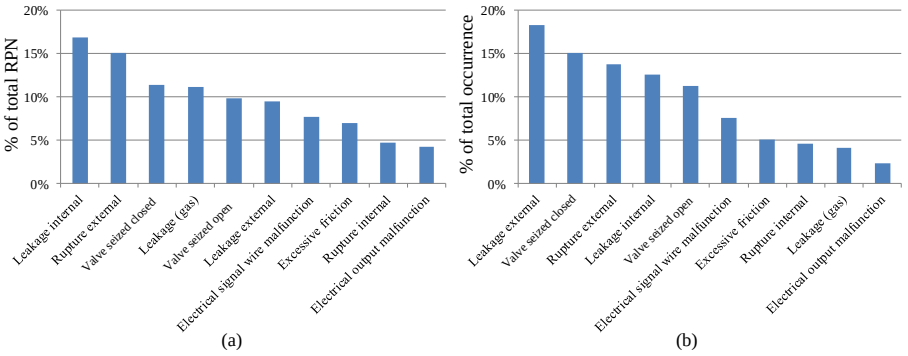

Fig. 3.4: Failure mode Pareto charts for top 10 risks (a) and occurrence (b).

The Pareto chart in Fig. 3.5 (a) shows the top 10 root causes for the pitch system in relation to risk. The three top root causes lead to leakage in the system and are closely related to the system and component design. With the exception of connection failure and electrical actuator malfunction, the remaining root causes are associated with the fluid condition and are resulting in loss of valve control or seizure. This highlights the necessity of ensuring high quality of the fluid in order to mitigate many of the faults seen in pitch systems. The Pareto chart in Fig. 3.5 (b) confirms that the fluid condition likewise has an impact on reliability. However, the fluid condition is not investigated further in this thesis.

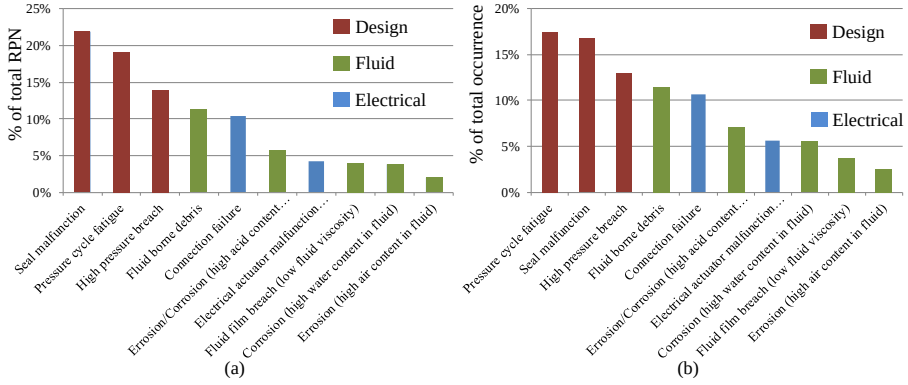

Fig. 3.5: Root cause Pareto charts for top 10 risks (a) and occurrence (b).

Conclusively, the design tool emphasizes issues generally applicable to fluid power systems such as leakage and low quality fluid condition. However, specific concerns such as accumulator gas leakage and electrical actua-

tor malfunction also show to introduce both high risk and lowered reliability. Additionally, the design tool offers the ability to directly evaluate the relative impact of design changes and implementation of condition monitoring methods. To show an effect of how the tool may be used, an alternative fluid power pitch system concept is evaluated in the following section.

3.3 Comparative Study of Pitch System Concepts

With the application of the design tool, two concepts are compared in this section and evaluated with respect to risk and reliability. This section is based on the work presented in paper D.

Pitch System Concepts

The results from a review of different pitch system concepts conducted in paper A showed that multiple concepts are proposed with the objective of increasing reliability. The review focuses on concepts predominantly evident from patents and patent applications. The review showed that many propose closed-reservoir type stand-alone cylinder drives fully contained in the hub. However, there is no record of physically testing of these systems. Despite this, several advantages arise from these concepts such as the elimination of a high-pressure leakage path through the rotary union (R1). The single point of failure caused by the conventional common HPU is also mitigated at the cost of increasing the component count. The increased component count potentially also yields more faults and therefore a reduced reliability.

The two systems compared are the conventional concept as given in Fig. 2.1 and the bootstrap (pressurized closed reservoir) concept shown in Fig. 3.6. The proposed bootstrap concept utilizes the same actuation circuit as used for conventional type systems, thus only the supply diagram is shown in Fig. 3.6. The differences lie in the closed-type stand-alone configuration facilitated by a bootstrap reservoir. The bootstrap reservoir is normally used in the aviation industry where the function of the systems is needed irrespective of the orientation. This allows for the bootstrap to be fully contained in the rotating hub. The bootstrap uses supply pressure to generate a reservoir pressure slightly above the atmospheric pressure for feeding the suction side of the pump. Note that one bootstrap supply is used for each pitch actuator in the proposed alternative system.

Results

Figure 3.7 (a) shows the RPN normalized w.r.t. the conventional concept. The RPN for both concepts is seen to similar which indicates that the safety integrity of the systems is equal. The RPN is divided into operational modes.

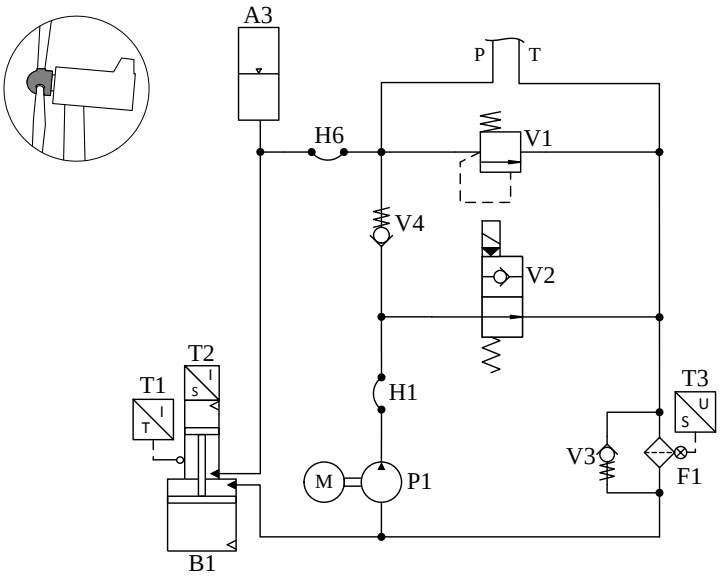

Fig. 3.6: Bootstrap supply for a single pitch actuator. The entire pitch system is contained in the rotating hub. Figure from paper D.

Single power regulation fault describes the fault of one out of three pitch systems not being able to adjust the pitch angle in normal operation. The bootstrap is robust to start-up and 2oo3 emergency shutdown faults due to the elimination of the single point of failure caused by the common HPU in the conventional concept. 2oo3 emergency shutdown fault refers to at least two out of the three pitch systems not being able to perform accumulator powered extension of the pitch cylinders. As mentioned before, modern wind turbines are normally designed with such redundancy allowing the emergency shutdown system of one blade to fail while still bringing hub rotation to a halt.

Figure 3.7 (b) shows the occurrence of both systems normalized w.r.t. the conventional concept. The occurrence of faults is seen to be highest for the bootstrap concept which consequently yields the lowest reliability. A study of the individual components in paper D shows that the increased number of pumps and valves in the supply circuit significantly increase the occurrence of failures for the bootstrap concept. A further study conducted under the assumption of a single hub-contained common bootstrap supply reveals a slight reduction of both the RPN and occurrence compared to the conventional concept. Such concept is associated with the same single point of failure as valid for the conventional system but without the high-pressure leakage path caused by the rotary union. A pitch concept based on a com-

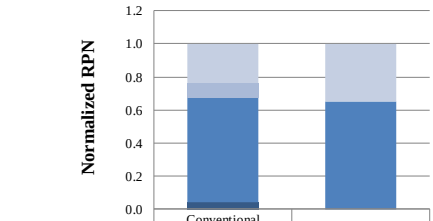

	Conventional concept	Bootstrap concept
Single power regulation fault	23.7%	34.6%
Start-up fault	8.9%	0.0%
Single emergency shut down fault	62.9%	65.1%
2oo3 emergency shut down fault	4.5%	0.0%

(a)

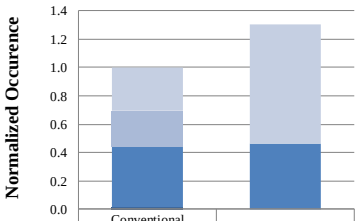

	Conventional concept	Bootstrap concept
Single power regulation fault	30.6%	84.2%
Start-up fault	25.4%	0.0%
Single emergency shut down fault	42.9%	46.6%
2oo3 emergency shut down fault	1.1%	0.0%

(b)

Fig. 3.7: Conventional and bootstrap comparison in terms of risk (a) and occurrence (b). Figure from paper D.

mon bootstrap supply fully contained in the hub may, therefore, be relevant for a further investigation.

It is noted that the analysis did not consider the cost of components, manufacturing, installation, and maintenance. Since the bootstrap concept needs no fluid connection between the nacelle and hub, the installation and main shaft manufacturing costs may be lowered in relation to the conventional concept.

3.4 Quantitative Analysis

The quantitative analysis differs from the previously presented qualitative analysis by utilizing component failure rates or reliability probabilities for assessing the system risk and reliability. Given that such component information is available, the quantitative analysis has the potential to greatly reduce the bias and subjectivity issues related to qualitative based analysis. This section presents a feasibility study of a failure rate estimation procedure for fluid power components based on the work presented in paper C.

State of the Art

Two studies specifically considered the reliability assessment of fluid power pitch systems [32, 95]. In [95], Yang et al. utilized a Stochastic Petri Net (SPN) for a fluid power pitch system of a Vestas V39 turbine. The SPN was first used for analyzing fault propagation and finally for determining reliability through the minimal cut-set of the system. The minimal cut-set presents the

least number of events linking fault to pitch systems failure. The determined system failure rate amounted to 0.75 failure pr. year, which is slightly less than what is found in the field data presented in Fig. 3.1. The origin of the failure probabilities used in the study was however not evident. It is also worth noting, that only a very limited number of failure modes were considered in the study. Han et al. similarly presented reliability modeling of the Vestas V39 turbine, but utilized an FTA and translating to an SPN for analyzing fault propagation [32]. Again, only a very limited number of failure modes were considered and no information on failure rates was given. Evidently, reliability assessment of pitch systems has mostly been focussed on modeling methods rather than establishing the quantitative basis.

As given in a review in paper A, only the *Handbook of Reliability Prediction Procedures for Mechanical Equipment* covers failure rates estimation in relation to fluid power components [47]. The procedures of the handbook are utilized in the following section for estimating component failure rates and subsequently correlated to field data.

Failure Rate Estimation

The failure rate models given in [47] are divided in sub-components as seal, seat-land interface, spring, etc. A component failure rate estimate is determined as the sum of the failure rates of sub-components. The sub-component failure rate are constructed from an empirical base failure rate, λ_B, multiplied by several non-dimensional multiplication factors. An example of failure rate estimation for a poppet in a seat type valve is given in Eq. (3.3).

$$\lambda_{poppet} = \lambda_{B,poppet} C_p C_q C_f C_v C_n C_s C_{dt} C_{sw} C_w \frac{N_{cycle}}{t_H} \tag{3.3}$$

where the multiplication factors are described in Table 3.2. $C_p, C_q, C_v, C_n, C_s, C_w$

Table 3.2: Multiplication factor description for seat type valve.

Factor	Description
C_p	Pressure drop factor
C_q	Allowable leakage factor
C_f	Surface finish factor
C_v	Fluid viscosity factor
C_n	Fluid contamination factor
C_s	Contact pressure factor
C_{dt}	Seat diameter factor
C_{sw}	Land width factor
C_w	Flow rate factor

depends on operating pressure, flow, fluid viscosity, and allowable leakage.

C_f, C_{dt}, C_{sw} are design dimension and manufacturing depended multiplication factors. $\frac{N_{cycle}}{t_H}$ is valve cycles per hour. Further details on the multiplication factors are given in paper C.

Pressures, flow and valve cycle rates are determined by simulation of the model presented in section 2.3. The validity of the results is evaluated by comparing the estimated failure rates to the field failure rates from the study by Carroll et al. [15] as given in section 3.1. However, the operation conditions such as wind speed, turbulence intensity, and temperatures are unknown for the real-life turbines used in the field study. Therefore, a wide range of operating conditions is used in the simulations for generating a span for the estimated failure rates which are correlated to the field data.

Among others, a parameter study is conducted on the travel threshold determining when a cycle is counted for both the proportional valve, the cylinder and the accumulators. The travel threshold is one of the most influential parameters on the estimated failure rates. The grouped failure rates for a range of travel thresholds are seen in Fig. 3.8. The black bars indicate the span of the simulated results for the considered range of wind speeds and turbulence intensities.

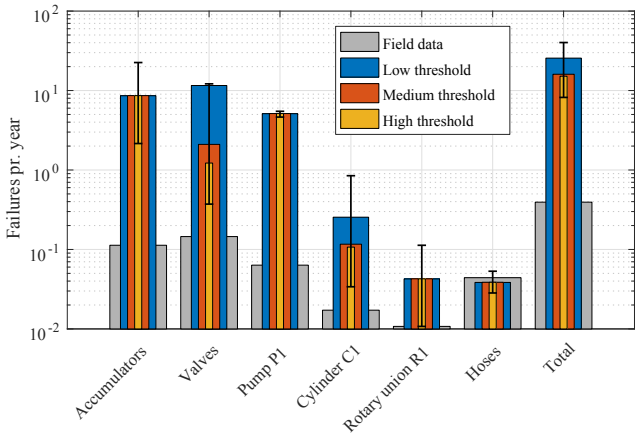

Fig. 3.8: Component group failure rates for three levels of travel thresholds. Other conditions are $T_{amb} = 20°C$ and $T_{fluid} = 50°C$. Black bars indicate the full span of the simulated results. Figure from paper C.

The estimated failure rates are, except for hoses, at least an order of magnitude larger than the field data. While increasing the travel threshold lowers the failure rates, the results are unsatisfying. Hoses present the only component group where field data are within the span of estimated values.

At low travel threshold, the estimated failure rates for all component groups except hoses, are seen to follow the same tendency as the field data.

However, deviating by orders of magnitude. Indications are therefore that the estimation procedure for fluid power components provided in the *Handbook of Reliability Prediction Procedures for Mechanical Equipment* is generally over-conservative. This could be a consequence of the empirical basis for the procedures which in some cases dates back to the late 1960's. The latest improvement in component design, manufacturing processes, and fluid quality is therefore not considered. Hence further work, especially on reliability testing of newer components, are needed to increase the precision of the failure rate estimation procedure.

Conclusively, the state-of-the-art method for quantitative reliability assessment is not able to generate a usable estimate for fluid power pitch systems. Currently, the best reliability estimate is therefore provided by the qualitative design tool presented in Section 3.2.

4 Fault Detection & Diagnosis

In this chapter, the high risk and reliability reducing faults for the pitch system are investigated in terms of FDD. A general review is given on methods utilized in pitch systems. This is followed by a presentation of FDD methods for two specific component types, namely, the accumulator and solenoid valve.

4.1 Fluid Power Pitch FDD Methods

As given in the review in paper A, Odgaard et al. [73] and Shi et al. [85] developed FDD methods specifically for fluid power pitch systems covering faults from a drop in supply pressure and lowered fluid bulk modulus. Similar faults, including pitch angle sensor fault, were considered in the fault-tolerant scheme by Chen et al. [16]. The fault-tolerant scheme enabled synchronization of blade pitch angles even in the event of a pitch angle sensor fault. Thus, mitigating unbalanced structural loads. The aforementioned references all assumed that the pitch system dynamics may be modeled as a linear second-order system and only presented results based on simulations. Further work is therefore needed for proving the methods for real pitch system dynamics. Experimentally validated fault detection methods are presented by Choux et al. [17] and Wu et al. [94]. Both developed detection methods for internal and external leakage for pitch cylinders and the experimental results are promising.

However, in relation to risk and reliability, neither of the faults considered in the previous works are critical. In Chapter 3, high-risk faults in fluid power pitch systems showed to be valve seizure, leakage and accumulator gas leakage. As pointed out in paper B [Fig. 10], the top contributors to the risk are components V7, V8, and A1 or A2 which are all related to the emergency shutdown operating mode. Two patent applications deal with these critical components through testing of the emergency function. Nielsen et al. [70] proposed a method for detecting the ability of the accumulator to supply a sufficient amount of fluid for an emergency stop of a wind turbine. The method utilized an extra orifice connected between the accumulator and

tank via an on/off valve. However, the connection of these additional components introduces further risk to the system. Minami et al. [69] and Yuge et al. [96] presented methods for testing performance of the emergency shutdown system. The methods rely on performing an actual emergency shutdown procedure, thus limiting the utilization of the wind turbine for power production.

All in all, the methods available for fault detection in critical components either increase risk or prevent the turbine from being operated while testing. The FDD methods presented in the following sections are therefore developed with special attention to online fault detection and applicability in existing pitch system designs. Early detection of faults is also considered to be an important design objective. Thus, aiding to do condition-based maintenance, with the potential to reduce downtime.

To give an overview, the design tool presented in Section 3.2 has been utilized to analyze the effect of six detection scenarios. Figure 4.1 shows the result. Both the reduction of the RPN and the summarized occurrence score is given for each scenario.

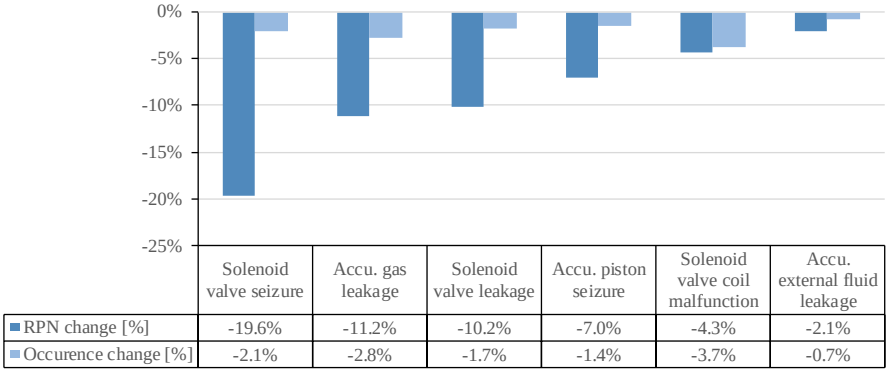

	Solenoid valve seizure	Accu. gas leakage	Solenoid valve leakage	Accu. piston seizure	Solenoid valve coil malfunction	Accu. external fluid leakage
RPN change [%]	-19.6%	-11.2%	-10.2%	-7.0%	-4.3%	-2.1%
Occurence change [%]	-2.1%	-2.8%	-1.7%	-1.4%	-3.7%	-0.7%

Fig. 4.1: RPN and occurrence reduction for FDD applied to critical faults in fluid power pitch systems.

The scenarios build on the assumption that an FDD method is designed to facilitate early detection of the fault such that it can be mitigated before system failure. Thus, leading to a reduction of the occurrence and detection scores to the lowest possible values. Additionally, the FDD methods are assumed to be applied directly to conventional pitch systems without changing the layout. Solenoid valve leakage detection is only considered for critical components V7 and V8, while valve seizure and coil malfunction detection are applied to all solenoid valves. It should be noted, that the change in percentage-values presented in Fig. 4.1 are only to be interpreted rela-

tively. That is, the percentage-values indicate the relative significance to risk and reliability. The actual impact to reliability must be determined through quantitative studies.

Figure 4.1 shows that the most significant risk reduction is possible through detection of valve seizure followed by accumulator gas leakage detection. The largest reduction of occurrence is facilitated by detection of a coil malfunction in solenoid valves. Detection of accumulator gas leakage and solenoid valve malfunction is, therefore, investigated in the succeeding sections.

4.2 Solenoid Valve FDD

According to several studies [4, 45, 52, 67, 92], failures in solenoid valves can be divided into three main groups, namely, coil malfunction, valve leakage, and plunger/poppet seizure. As given from Fig. 4.1, the prevention of seizure shows to have the most potential for lowering the risk of the pitch system.

Much literature is available on detection of faults related valve seizure. A feasibility study of different approaches is conducted by Kryter on monitoring of solenoid valves in operation [54]. Perotti et al. [77] utilized the back-emf signature in a coil current measurement during operation for detecting partial and seized plunger movement. Among others, Khoshzaban-Zavarehi [52], Börner et al. [11], Jouppila et al. [51], and Dülk et al. [18] presented model-based methods using coil voltage and current during operation for plunger position estimation, which is also applicable for detection of plunger movement failure. The ability of these methods for detecting the early signs of failure is, however, not evident and the fault to failure progress has not been investigated. Characterization of plunger movement degradation is presumably dependent on many operational circumstances such as fluid quality, temperature, pressure, flow, etc. Such characterization, therefore, requires significant experimental effort and the plunger movement degradation is not investigated further in this thesis.

In relation to valve leakage, Khoshzaban-Zavarehi [52] presented valve leakage detection using measured plunger position and valve pressure drop. Simple one-way solenoid valves as those conventionally used in pitch systems are not equipped with a plunger position sensor or pressure sensors. Such sensors are expensive, and the method is therefore only considered useful when the added cost can be justified. Valve leakage detection is therefore neither considered further in this thesis.

From a pitch system reliability perspective, the most significant gain is achieved by monitoring of coil malfunction. The significance of coil malfunction is likewise emphasized in a study by Oak Ridge National Laboratory (ORNL) based on data from the Nuclear Plant Reliability Data System

(NPRDS) [4]. Coil malfunction is shown to be the most dominant failure for solenoid valves operated in nuclear plants. The detection of insulation degradation in solenoid valves was investigated by Jameson et al. [44] by utilization of high-frequency impedance change. High-frequency was assessed by measuring coil current as a result of superimposing the DC control voltage with a high-frequency component. Experiments showed changing impedance due to insulation degradation under isothermal conditions. It was also noted, that the high-frequency impedance changes more significantly than fault induced changes in the coil resistance. Further experimental work by Jameson et al. [44, 46] showed the possibility of using the method for distinguishing between faults caused by thermal and chemical degradation. The method seems promising for online detection of early signs of coil failure. However, as noted by Jameson et al. [44], no indication is given on the temperature robustness of the method. Temperature robustness is considered to be very important, as coils operated in wind turbines are exposed to a wide range of temperature conditions. The main objective of the following is, therefore, to present a temperature robust method for detecting the early signs of coil failure.

Early Detection of Coil Failure

The following is based in the work presented in paper G. Several accelerated test were conducted for characterizing insulation break down in the coil package of solenoid valves. The tests were carried out at an ambient temperature of 190°C which caused coil failure in 24 to 48 hours of operation. A fault is defined as a relative resistance change according to:

$$\Delta R_{ref} = \frac{U_C}{1 + \alpha \left(T_C - T_{ref} \right)} \left(\frac{1}{i_{post}} - \frac{1}{i_{prior}} \right) \tag{4.1}$$

where U_c is the terminal voltage, T_C is the coil temperature, and i_{prior} and i_{post} are coil current measured directly before and after a fault instance respectively. α is the temperature coefficient of resistance for copper. $T_{ref} = 20°\text{C}$ is selected as reference to compensate for coil temperature. The relative resistance change is purely due to convenience defined positive for a reduction in absolute resistance of the coil.

The effect of continuous operation versus a modulated on/off signal pattern is investigated. Figure 4.2 shows the fault instances as a function of the fault size given by the relative resistance change ΔR_{ref}. During the tests, all faults were seen to occur as rapid steps in coil current. The first instances of fault were present at 50-80% of the remaining lifetime which emphasizes the possibility of early detection. This behavior was likewise confirmed in the experimental study by Angadi et al. [1].

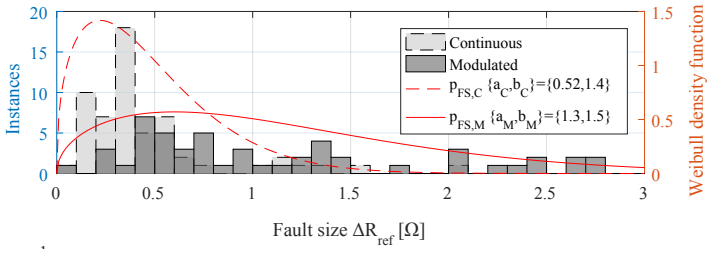

Fig. 4.2: Fault size histogram and statistics for both continuous and modulated excitation signals. Figure from paper G.

Clearly, for the fault size for solenoids that are operated continuously is lower compared to the fault size occurring for solenoids operated by a modulated signal. In either case, typical fault sizes are less than 5% of the nominal 15Ω coil resistance. It should be noted that the resistance change due to a coil temperature change of just 5°C is similar to the typical fault sizes. Evidently, detection must be robust to temperature changes for isolation of coil faults. The Weibull distribution is used for further statistical analysis and the shape b and scale a parameters are given in the figure.

Figure 4.3 shows the number of faults before failure N_{FI} for the tested solenoids.

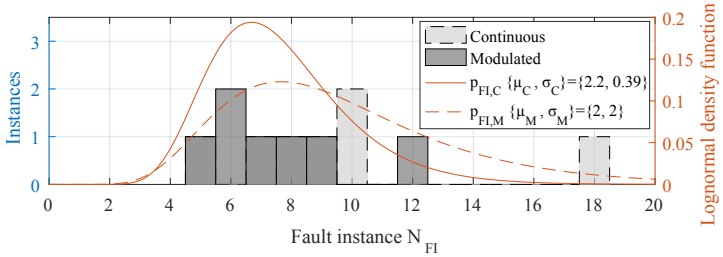

Fig. 4.3: Fault instance histogram and statistics for both continuous and modulated excitation signals. Figure from paper G.

For all tested solenoids, at least five fault instances before failure are observed. Continuously operated solenoids are exhibiting slightly more faults than a modulated solenoid. The lognormal distribution is used for further statistical analysis and the mean μ and standard deviation α parameters are given in the figure.

Detection Method

An overview of the detection method is shown in Fig. 4.4. The diagram shows an EKF utilizing thermal models of solenoid valves and the steel man-

ifold block to which the valves are connected. The EKF is chosen due to its applicability in nonlinear and stochastic systems for estimating states recursively. For linear and fully observable systems, the Kalman Filter (KF) presents an optimal state estimate for known model uncertainty and signal noise distributions. The EKF uses linear first-order approximations of the non-linear system model and, therefore, do not present the optimal state estimate. However, a precise estimate is obtained for systems that are well described by linearization at each operation point [35]. This can be obtained, for instance, by selecting a sampling time sufficiently smaller than the system dynamics. A sampling time of 0.5s showed sufficient for proper detection. It is noted, that the sampling time is orders of magnitudes higher than needed for coil fault detection methods presented by Jameson et al. [44, 46]. Also, the method presented in this thesis does not rely on additional high-frequency excitation which permits implementation on low-cost equipment. Further information on the implementation and tuning of the EKF is found in paper G.

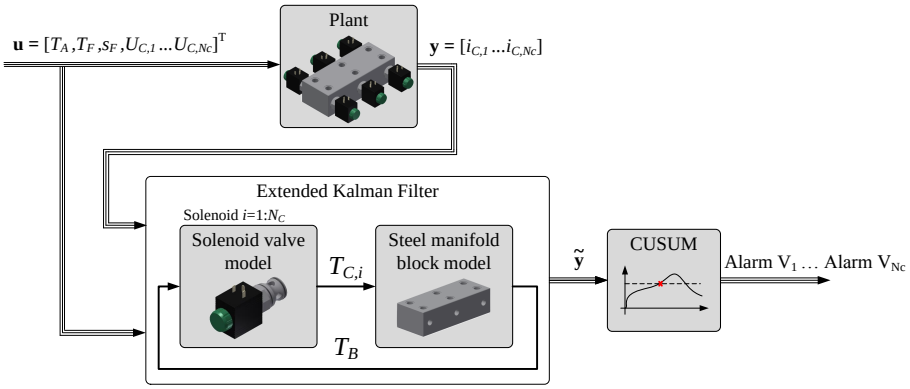

Fig. 4.4: Diagram of the method for detecting the early signs of coil failure.

The input $\mathbf{u}$ to the EKF is the ambient temperature T_A, fluid temperature T_F, flow signal s_F, and coil voltages $U_{C,1} \dots U_{C,N_C}$. N_C is the number of solenoid valves connected to the steel block. All inputs are normally available in conventional pitch systems.

The measured output $\mathbf{y}$ consists of the coil currents $i_{C,1} \dots i_{C,N_C}$. The coil currents are normally not available in pitch systems, however, they can simply be measured at the controller output.

The thermal behavior of the coils are described by lumped parameter models of the solenoid and steel block. As shown in paper G, the steel block temperature significantly influences the coil temperature. A model of the steel block is therefore necessary since no temperature measurement is available in pitch systems. The thermal behavior of the ith solenoid and the steel

block is described in Eq. (4.3) and Eq. (4.5) respectively. The notation and sign convention are given in Fig. 4.5.

$$\dot{T}_{C,i}\, c_{pC}\, m_C = \dot{Q}_{j,i} - \dot{Q}_{CB,i} - \dot{Q}_{CA,i} \tag{4.2}$$

$$\Rightarrow \dot{T}_{C,i} = \frac{{U_{C,i}}^2}{K_C\, R_{ref}\left(1+\alpha\left(T_{C,i}-T_{ref}\right)\right)} - \frac{T_{C,i}-T_B}{\tau_{CB}} - \frac{T_{C,i}-T_A}{\tau_{CA}} \tag{4.3}$$

$$\dot{T}_B\, c_{pB}\, m_B = -\dot{Q}_{BA} - s_F\, \dot{Q}_{FB} + \sum_{i=1}^{N_C} \dot{Q}_{CB,i} \tag{4.4}$$

$$\Rightarrow \dot{T}_B = -\frac{T_B - T_A}{\tau_{BA}} - s_F\, \frac{T_F - T_B}{\tau_{FB}} + \frac{1}{\tau_{BC}} \sum_{i=1}^{N_C} T_{C,i} - T_B \tag{4.5}$$

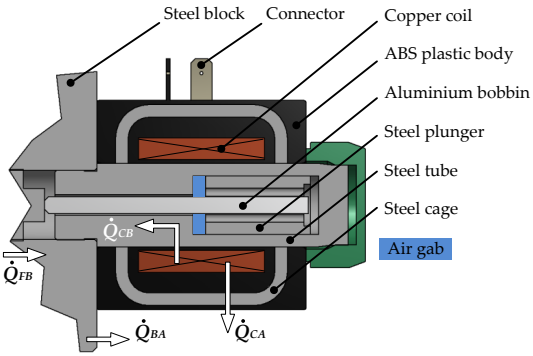

Fig. 4.5: Section view of a convention solenoid valve mounted in a steel manifold block. Nomenclature and positive conventions for heat transfer are indicated by arrows. Figure from paper G.

All constants $\{K_C,\, R_{ref},\, \tau_{CB},\, \tau_{CA},\, \tau_{BA},\, \tau_{FB},\, \tau_{BC}\}$ are estimated from the experiments described in paper G.

Detection is performed by residual evaluation using the CUmulative SUM (CUSUM) method. The CUSUM is used for detecting when a process mean deviates from a preset threshold [5]. An alarm is set when a certain amount of samples have deviated above the preset threshold. In the experiments, the thresholds are selected as low as possible without yielding false alarms. A coil fault corresponds to an increase in residual. Hence, the upper CUSUM is used for detection.

Experimental Results

The detection method is experimentally validated by using the setup shown in Fig. 4.6. The setup consists of a steel manifold block with three 4/3 way

solenoid valves. The ports of valve V1 and V2 are blocked and valve V3 controls flow through the steel block. The setup allows for injecting faults to Valves V1 and V2 by connecting a resistor in parallel with the coil terminals. Consequently, the equivalent coil resistance drops similarly to a coil fault. The fault size is adjusted through selection of different parallel resistors.

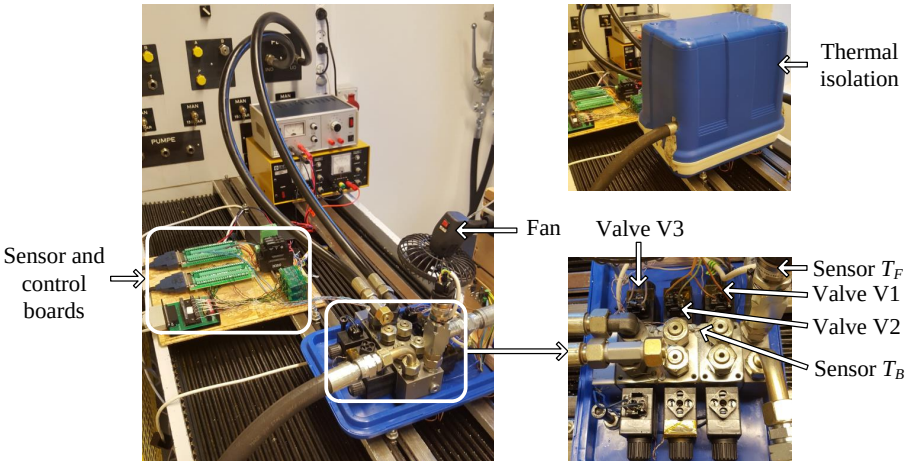

Fig. 4.6: Overview of the experimental test setup used for model validation and fault detection.

The experiments are performed for a predefined test scenario where the fluid flow, convention conditions, and the ambient temperature are varied. All model constants are estimated under free convention conditions. Air flowing past the steel block and solenoids causes forced convection and therefore acts as a disturbance to the model. A fan is installed directly over the steel block as shown in Fig. 4.6 for testing robustness of the detection method in different convection conditions.

The ambient temperature is varied by covering the steel block and valves with a thermal isolation box. When covered, the ambient temperature increases due to heating by the fluid and heating by the solenoids. The test scenario is shown in Fig. 4.7. The isolating box is removed after the first two hours, which causes a rapid drop in ambient temperature. The fan is simultaneously turned on leading to fast cooling of the solenoids. Subsequently, the coil resistance drops similarly to a coil fault which enables robustness testing of the detection method under such conditions. The four-hour test scenario leads to at least one repetition of each combination of the conditions. During the tests, valve V1 is operated intermittently and valve V2 is continuously turned on. The fault characteristics for intermittent and modulated operating are assumed to be similar. The intermittent operating signal is chosen as it causes high coil temperature changes due to a varying duty cycle. This allows for further testing the temperature robustness of the detection method.

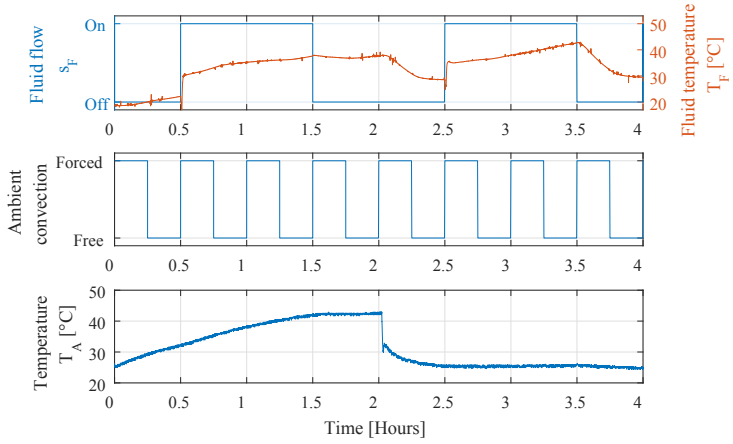

Fig. 4.7: Ambient temperature, convection and flow conditions used in the test scenario. Figure from paper G.

The first 10 minutes of a test is shown in Fig. 4.8. The top graph shows

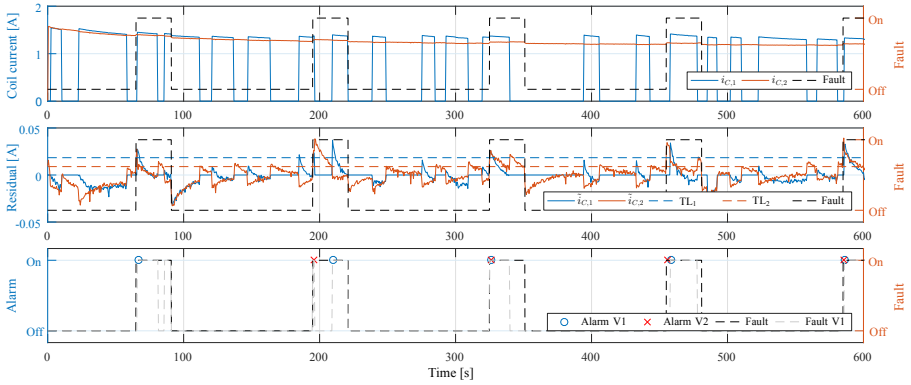

Fig. 4.8: First 10 minutes of the test scenario where faults are injected periodically. Figure from paper G.

the measured coil currents and state of the injected fault. The coil currents expectedly show a minor increase when the fault is active. The middle graph shows the coil current residuals including the selected CUSUM thresholds TL_1 and TL_2. The ability of the method to detect faults is evident from the bottom graph. The gray dashed line indicates when both the fault and valve V1 are active, which permits detection. All faults are detected for valve V1, while the first fault instance is missed for valve V2. This behavior is caused by low model accuracy during the initial part of the test scenario where the coil temperature increases significantly due to coil heating. It is noted, that

decreasing the CUSUM thresholds allowed for detection of this fault. This, however, increased the number of false detections. Detection of this initial fault is not pursued further since continuously operated valves only exhibit significant coil heating during the first minutes of operation. Afterwards, fault detection shows reliable results and detects all injected faults.

The lowest reliably detectable fault sizes for continuous and intermittent operation are given as $\min(\Delta R_{ref})$ in Table 4.1. The lowest reliably detectable fault sizes are found for the continuously operated solenoids.

Table 4.1: Detection probability for minimum detectable fault sizes. Based on table from paper G.

		Fault instance N_{FI}		
Detection probability	$\min(\Delta R_{ref})$	1	2	3
Intermittent	0.36Ω	0.86	0.98	0.996
Continuous	0.26Ω	0.69	0.90	0.97

The detection probabilities are determined from the statistical distributions given in Fig. 4.2 and Fig. 4.3. The highest detection probabilities are present for the intermittently operated solenoid valves even though the minimum detectable fault size is larger than for continuously operated valves. As seen in Fig. 4.2, this is a consequence of the fault sizes generally being larger in intermittent operation. All in all, the detection probabilities are regarded as very high. At least 97% of faults are detected at third instance. This conclusion also takes the detection time into account. The detection time is defined as the time from injected fault to detection. The experiments show mean detection times below 2s which is generally much faster than the fault develops. The proposed method is, therefore, able to reliably detect coil faults before failure.

4.3 Accumulator FDD

This section presents the development and application of a detection method for one of the high-risk faults in pitch systems, namely accumulator gas leakage.

A few methods where presented in Section 4.1 on monitoring of the accumulator function in pitch systems [69, 70, 96]. However, the methods rely on either additional risk-increasing equipment or turbine shutdown. Accumulator gas leakage may accurately be estimated by having knowledge of the gas temperature, piston position, and fluid pressure. Intrusive methods for measuring the piston position suggested in patents [30, 53, 75]. However, adding a sensor connected to the inside of the accumulator introduces external leakage paths and increases risk. Non-intrusive piston measurement

using inductive sensors on the accumulator surface was suggested by Bauer et al. [6]. No additional sensors are needed in the method proposed in a patent by Hosada et al. [41]. The latter method applies to a system similar to the supply unit in wind turbines. It utilizes the pump duty cycle which decreases when a gas leakage occurs. In pitch systems, the pump duty cycle is, however, also highly dependent on load flow to the pitch cylinders. The method is, therefore, not directly applicable. Helwig et al. [36] presented a signal-based method for detection of various faults in a hydraulic system including accumulator gas leakage. The method uses linear discriminant analysis of time domain features from multiple measurements of pressures, flow, and temperature. The method has shown excellent experimental results for periodic excitation of the system. However, precision has been shown to decrease drastically for pseudo-random excitation. This poses a problem for pitch systems due to the random loading conditions caused by changing wind speeds and turbulence. A State-of-Charge (SoC) estimator for an accumulator in hydraulic hybrid vehicles was proposed by Pfeffer et al. [78]. The estimator is based on an EKF using fluid pressure, gas temperature, and estimated pump flow as input. Gas leakage has not been directly investigated, however, the gas mass was introduced in a joint state and parameter estimation scheme. A reduction of gas mass will indicate a gas leakage. Experimental results showed a precise estimation of gas mass, but no indication is given on the precision in the event of gas leakage. In addition, the method uses a gas temperature sensor which is not present in accumulators used in wind turbines.

Therefore, two methods for detecting accumulator gas leakage are investigated in the following sections. A signal-based method using only the fluid pressure sensor signal for fault feature extraction. This is followed by a model-based method utilizing the EKF similar to the approach suggested by Pfeffer et al. [78], but eliminating the need for a gas temperature sensor.

Fault definition

Both internal and external gas leakage reduces the ability to perform an emergency shutdown. Thus, both are considered as a gas leakage fault. Internal gas leakage occurs via the piston seal to the fluid side of the accumulator. Internally leaking gas is assumed to be transported with the fluid to the reservoir.

Gas leakage is normally a very slow process developing over weeks or months. Hence, instead of considering the gas leakage itself, it is normal to consider the amount of remaining gas in the accumulator. It is convenient to use the pre-charge gas pressure when the accumulator holds no fluid as an indicator of remaining gas. The pre-charge pressure is dependent on the gas temperature and all further values are evaluated at $T_{pc} = 22°\text{C}$. In wind tur-

bines, a pre-charge pressure of 50–70 bar is normally considered as a lower threshold, however, the threshold strongly depends on the turbine configuration. The robustness of the proposed detection method is further evaluated in the event of fluid leakage occurring in the flow path between valve V4 and V11. An overview of the considered faults is given in Table 4.2.

Table 4.2: Main data for the considered faults. Table from paper E.

Fault	Measure	Value	Condition
Gas leakage	p_{pc}	50 – 180bar	Pre-charge temperature $T_{pc} = 22°\text{C}$
Fluid leakage	q_{le}	Zero/low/high $0/0.05/1\frac{L}{min}$	Supply pressure $p_s = 200\text{bar}$

Signal-based Gas Leakage Detection

The method proposed in this section is based on the work presented in paper E. The method is suitable for accumulators mounted in configuration 1 as seen in Fig. 2.1. In this configuration, the accumulator is continuously used while the turbine is in normal operation. A 500-second window of the pressure signal, for a simulated nominal operating condition, and three levels of pre-charge pressure is seen in Fig. 4.9. The nominal operating condition is simulated using the model presented in Section 2.3 at rated wind speed, turbulence intensity class A and ambient temperature $T_a = 22°\text{C}$.

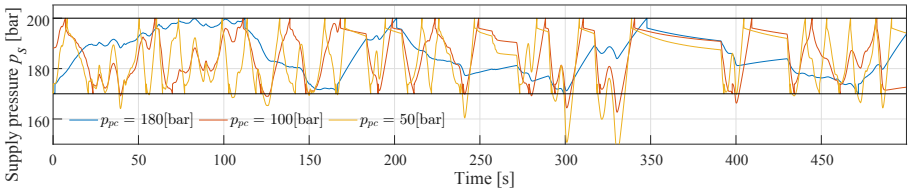

Fig. 4.9: Simulated supply pressure signal p_s, for three levels of pre-charge pressure in the nominal operating condition. Figure from paper E.

Recall, that the supply pressure is controlled in a simple on/off manner. Pump flow is dumped to the reservoir via valve V2 when an upper threshold of 200bar is reached. When the pressure decreases to the lower threshold of 170bar, the pump flow is redirected to the accumulator. Clearly, the frequency of these cycles increases when the pre-charge pressure decreases. This concurs with the diminishing ability to supply accumulator flow to the pitch cylinders when the amount of gas decreases. As mentioned, the on/off frequency is used in a patent by Hosoda et al. [41] for detection of gas leakage. However, it is not regarded a robust indicator of gas leakage since it

also depends heavily on the load flows Q_{v1}, Q_{v2}, Q_{v3}, which change for different wind speeds [76]. In Fig. 4.10, the frequency response of a linearized accumulator model shows increasing pressure oscillations due to a varying load flow input when the pre-charge pressure decreases. Thus, indicating

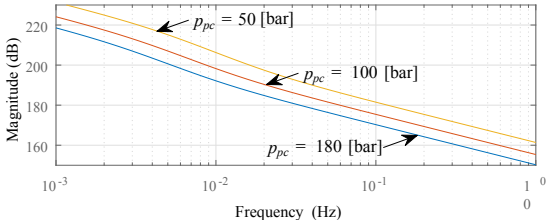

Fig. 4.10: Frequency response for transfer function $\frac{\Delta P_s(s)}{\Delta Q(s)}$ for three levels of pre-charge pressure. Operating point is set to $\bar{x}_0 = (p_{s0}, \dot{V}_{g0}, T_{g0}) = (185\text{bar}, 10\text{l/min}, 22^\circ\text{C})$. Figure from paper E.

that filtering of these pressure oscillations could indicate the presence of gas leakage. The motivation for the signal-based method, other than only depending on a single measurement, is to robustly filter out such fault features at different operating conditions.

Detection Method

The proposed method utilizes Multiresolution Signal Decomposition (MSD) based on the Wavelet Transform (WT) [64]. A similar approach has previously shown promising experimental results for detecting and isolating internal and external fluid leakage in actuators of fluid power cylinder drives [26, 27]. In comparison to the more commonly known Fast Fourier Transform (FFT), the WT adds the flexibility of choosing different mother wavelets for decomposition rather than just the sine wave. Selecting a mother wavelet that resembles the fault features allows for better filtering of the wanted characteristics [14]. This is confirmed as the WT has proven superior to FFT in comparative studies on fault detection in fluid power systems [21, 28].

An overview of the detection method is shown in Fig. 4.11, where the input is given simply by the supply pressure signal p_s.

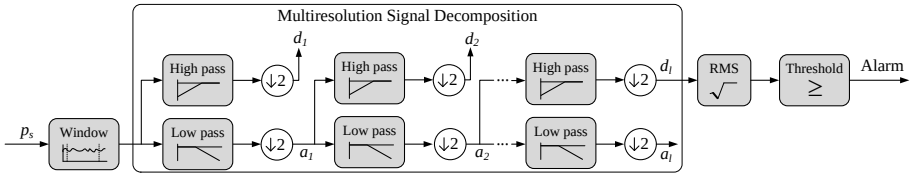

Fig. 4.11: Gas leakage detection using Multiresolution Signal Decomposition (MSD) of pressure signal p_s to the l-th level. Based on figure from paper E.

The pressure signal is feed to a cascade of Quadrature Mirror Filter banks (QMF) constructed by a pair of High Pass (HP) and Low Pass (LP) filters. Each HP and LP filter is based on the mother wavelet and generates detail d and approximation coefficients a respectively. The approximation coefficients are feed to the succeeding filter bank which facilitates next level approximation and detail coefficients. The signal is down-sampled by a factor of two at each level. The frequency content in the detail coefficients at l-th level decomposition is described by interval:

$$\left(f_{d_l\,\mathrm{Low}}, f_{d_l\mathrm{High}}\right) = \left(\frac{f_s}{4l}, \frac{f_s}{2l}\right) \tag{4.6}$$

where some overlapping occurs between the frequency bands. The overlapping is reduced by selection of higher order mother wavelets [25]. The sample frequency is selected to $f_s = 200$Hz. Previous studies used the eighth order Daubechies mother wavelet [26, 27], however, in comparison the fifth order Daubechies mother wavelet is found to be more sensitive to the gas leakage fault.

Simulation Results

As an example, Fig. 4.12 shows the level 9 detail coefficient of the pressure signal given in Fig. 4.9. The frequency band of detail coefficient level 9 is 0.39–0.78Hz.

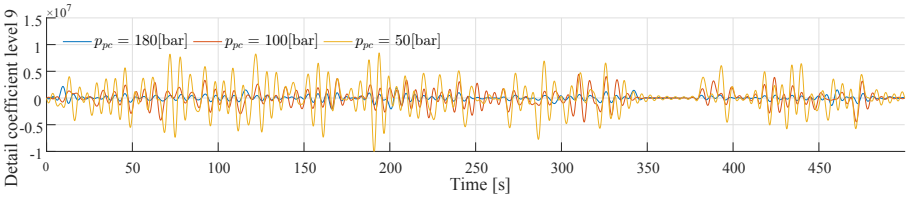

Fig. 4.12: Detail coefficient decomposition level 9 for three levels of pre-charge pressure in the nominal operating condition. Decomposed using the fifth order Daubechies mother wavelet. Figure from paper E.

The amplitude of the detail coefficient is clearly seen to increase for decreasing pre-charge pressure. Detection is facilitated by determining the Root Mean Square (RMS) of a predefined time window of the pressure signal and comparing to a threshold. The threshold must be determined from experiments using an accumulator with low pre-charge pressure. A similar approach has been used for fluid power actuators in the work by Goharizzi and Sepehri [26, 27]. However, this method poses issues with respect to selecting the size of the time window and ensuring robustness to other than the used nominal operating conditions. A window size of 500 seconds is found to be

a good compromise between fast detection and obtaining sufficient information in the signal for detecting the fault.

Robustness to different operating conditions is evaluated by simulating in intervals of conditions for the wind speed, turbulence intensity, and ambient temperature. Wind speed and turbulence intensity affect the load flow, thus influencing the pressure oscillations. The ambient temperature also influences the accumulator pressure dynamics. The mean wind speeds considered are 11.4m/s (rated), 13m/s and 19m/s. All wind speeds are above rated and below cut-off since some pitch activity is needed for generating excitation in the pressure signal. The turbulence intensity range cover both class A and C. The ambient temperature range is selected to $T_a : \{-20, 0, 22, 60\}^\circ$C. Results in paper E reveal the ambient temperature as the parameter, which mostly decreases the robustness of detection. Figure 4.13 shows normalized RMS mean and full range for three values of pre-charge pressures at three ambient temperature intervals. Mean and full-range of values are given based on all 216 combinations of simulated operating conditions including three levels of fluid leakage.

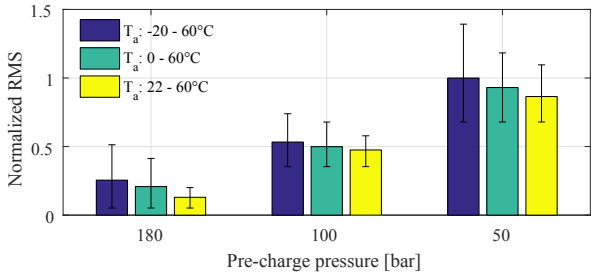

Fig. 4.13: Comparison between RMS mean and extreme values for reduced temperature ranges. The values are normalized with respect to the value at 50bar and temperature range -20–60°C. The error bars indicate the full range of RMS values.

Robust detection is permitted when the full range values do not overlap between the pre-charge levels. Reducing the ambient temperature range decreases the range of values and robust detection is possible in a temperature range of 22–60°C.

Detail coefficient level 9 is selected based on a study conducted in paper E, where it is shown to be the most sensitive to the fault and robust to different operating conditions. This concurs with a special disturbance occurring in the load flow to the accumulator at a frequency within the frequency band of detail coefficient level 9. The disturbance is caused by the tower effect, where local wind speed and direction for each blade is changed when the blade passes the tower. This generates load variation on the pitch actuator that propagates to the load flow. At nominal hub speed, the disturbance is induced at a frequency of 0.6Hz. In wind turbine terminology, this frequency

is denoted the 3P frequency. Which is, within the frequency band of detail coefficient level 9 at 0.39–0.78Hz. Therefore, the detail coefficient selected for accumulator gas leakage detection can preferably be chosen such that it covers the 3P frequency.

Experimental Results

The proposed signal-based detection method is experimentally validated on the test setup shown in Fig. 4.14.

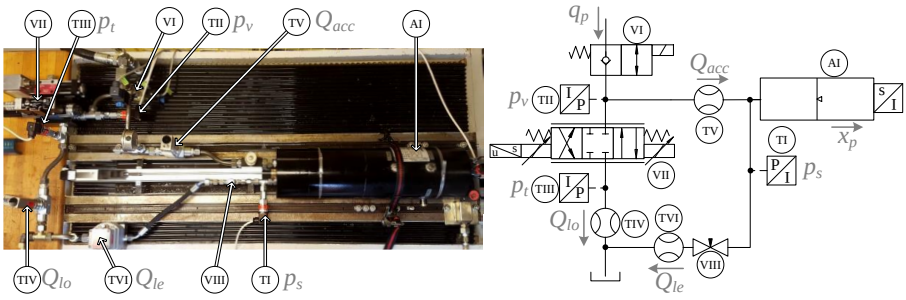

Fig. 4.14: Experimental setup and corresponding hydraulic diagram. Based on figure from paper E.

The test setup consists of a 6L piston type accumulator connected to a circuit for allowing operation similarly to the simulated conditions. The accumulator is equipped with a piston position sensor x_p in order to determine the actual gas volume. The load flow Q_{lo} is controlled (closed-loop) via proportional valve VII and flow sensor TIV to follow a scaled-down version of the sum $\sum_{i=1}^{3} Q_{v,i}$. The load flow is scaled in order to compensate for the reduced accumulator capacity of the setup (6L) compared to the simulated pitch system (50L). The scale factor is determined using the linearized model such that the magnitude of the pressure oscillations is similar for 6L and 50L accumulators. This likewise applies to the pump and leakage flows introduced in the setup. The pump flow is controlled similarly to the simulated system by toggling valve VI at high and low supply pressure levels. The leakage flow Q_{le} is introduced by opening the needle valve VIII and is measured using the flow sensor TVI.

A comparison of the simulation and experiment for nominal operating conditions and all three levels of fluid leakage is seen in Fig. 4.15. Each experiment is performed twice to ensure consistency, which yields a total of 24 experiments.

The experiments show a similar increase in RMS of the detail coefficient level 9 when the pre-charge pressure decreases until 75bar. The experiments are not as sensitive to a change from 75 to 50bar pre-charge pressure. Non-

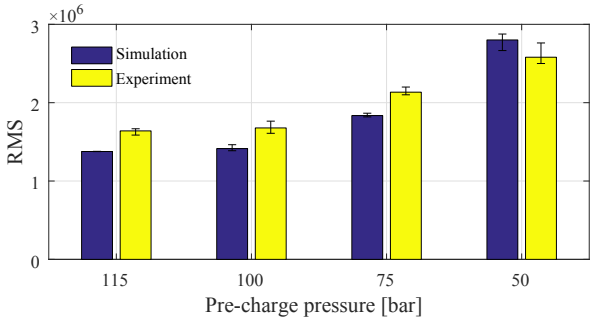

Fig. 4.15: Mean value of the detail coefficient RMS decomposition Level 9 using simulation and experimental data. The error bars indicate the full range of RMS values. Figure from paper E.

modeled factors such as flow restriction caused by flow sensor TV can be the cause of this discrepancy, however, more importantly, the RMS value at 50bar is still distinguishable from the 75bar pre-charge. The range of RMS values at each pre-charge pressure is slightly larger for the experiment than the simulation. Generally, the experiments show the feasibility of the method and confirm the robustness towards fluid leakage.

All in all, the method robustly detects changes in pre-charge pressures at operating conditions above rated wind speed and ambient temperatures above 22°C. Issues such as gas leakage detection at lower ambient temperatures and for accumulators mounted in configuration 2 is addressed in the next section.

Model-based Gas Leakage Detection

The method proposed in this section is based on the work presented in paper F. The method is model-based and amongst others, uses the ambient temperature as input for estimating gas leakage. The ambient temperature is introduced in order to address the lowered temperature range of the previously described signal-based method. The proposed method also encompasses gas leakage detection of accumulators mounted in configuration 2 as seen in Fig. 2.1.

Detection Method

Detection is facilitated by the use of an EKF and the accumulator model described in section 2.3. The reasoning for selecting a model-based method using the EKF generally follows a similar argumentation as given for solenoid coil fault detection in Section 4.2, i.e. the ability to incorporate non-linear dynamics. Also, the model-based method outputs an estimate of the pre-charge pressure which is more intuitive to interpret compared with the RMS value

of the signal-based method. However, the use of the model-based method introduces an additional requirement for sensors in the system compared the signal-based method. Namely the ambient temperature, piston velocity obtained from piston position, and pump state. These are all normally available in pitch systems. An overview of the detection method is given in Fig. 4.16.

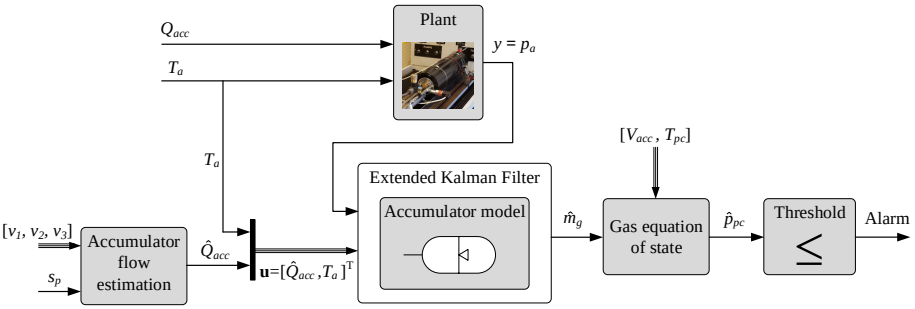

Fig. 4.16: Gas leakage detection using the EKF for joint state and parameter estimation.

The input of the EKF $\mathbf{u}$ is given by the estimated accumulator flow $\hat{Q}_{acc}$ and the ambient temperature T_a. While the ambient temperature is conventionally measured in pitch system, the input accumulator flow is not. An estimate derived from the available measurements is therefore constructed using the flow continuity given in Eq. (2.9). The relief valve flow can be assumed to $Q_{rel} = 0\text{l/min}$ for the entire supply pressure range in normal operation. The supply flow delivered by the fixed-speed fixed-displacement pump can be assumed to the nominal flow when the pump is on $Q_s = Q_{s,nom}\, s_p$ were s_p denotes a logic value representing the state of the pump as given in (2.8). The sum of flows to each actuation circuit $\sum_{i=1}^{3} Q_{v,i}$ can be estimated from the steady state assumption given in Eq. (4.7) where pressure build up flow between the pitch cylinder and proportional valve is neglected.

$$\sum_{i=1}^{3} Q_{v,i} \approx \sum_{i=1}^{3} A_{e,i}\, v_i \tag{4.7}$$

where v_i is the velocity of the ith pitch cylinder which can be found from numerical differentiation of the measured pitch position. $A_{e,i}$ denotes the effective piston area determined by:

$$A_{e,i} = \begin{cases} A_r & \text{for} \quad v_i > 0 \\ A_p - A_r & \text{for} \quad v_i < 0 \end{cases} \tag{4.8}$$

where A_p and A_r is piston and rod area respectively. The accumulator flow

estimation then yields:

$$\hat{Q}_{acc} = Q_{s,nom}\, s_p - \sum_{i=1}^{3} A_{e,i}\, v_i \tag{4.9}$$

Lastly, the EKF outputs the estimated gas mass $\hat{m}_g$ which is converted to the pre-charge pressure using the BWR equation of state given in Eq. (2.11), the pre-charge temperature T_{pc}, and the total accumulator volume V_{acc}. Further details on tuning and implementation of the EKF is given in paper F.

Experimental Results

Experimental verification is made on the same test setup as described in Section 4.3 page 50. A load sequence is constructed to cover operation of both accumulator configuration 1 and 2. The load sequence is shown in Fig. 4.17.

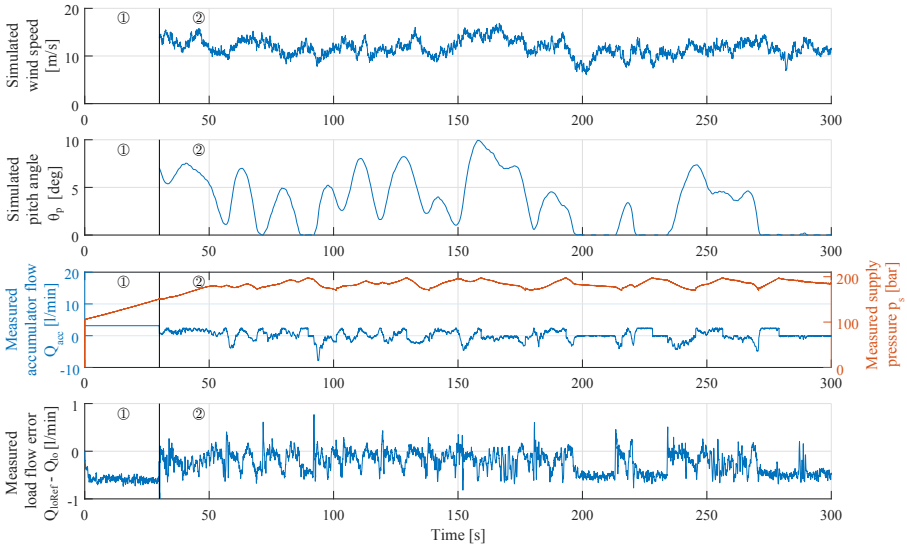

Fig. 4.17: Accumulator load sequence flow and supply pressure pressure. Accumulator pre-charge pressure is $p_{pc} = 100$bar. Figure from paper F.

The load sequence is divided into two regions. Region ① describes charging of the accumulators with fluid and is applied in both configuration 1 and 2 at startup of the wind turbine. The third plot from the top in Fig. 4.18 shows a constant positive accumulator flow and an increasing supply pressure. Region ① is active for 30s, after which the supply pressure reaches a sufficient level. Notice that a load flow error of -0.5l/min is seen in the bottom plot during region ① in Fig. 4.17. This is caused by an internal leakage from flow of the proportional valve VII, which could not be mitigated. The

leakage causes the actual accumulator flow Q_{acc}, to be smaller than estimated $\hat{Q}_{acc}$. Region ② describes normal operation in rated mean wind speed and is initiated instantly after region ① finalizes. The wind speed and corresponding pitch angle of one blade are shown in the two top graphs of Fig. 4.17. The load flow Q_{lo} is controlled closed-loop during region ② to match the simulated load flow. The control error is seen in the bottom graph of Fig. 4.17. As described, internal leakage causes the error to be mostly negative. The progress of the supply pressure is, however, very similar to the simulated values previously shown in Fig. 4.9.

Experimental results based on the load sequence and pre-charge $p_{pc} = 100$bar is shown in Fig. 4.18. The initial condition $\hat{m}_{g0} = 3 \cdot 10^{-5}$kg corresponds to a pre-charge pressure of 10bar.

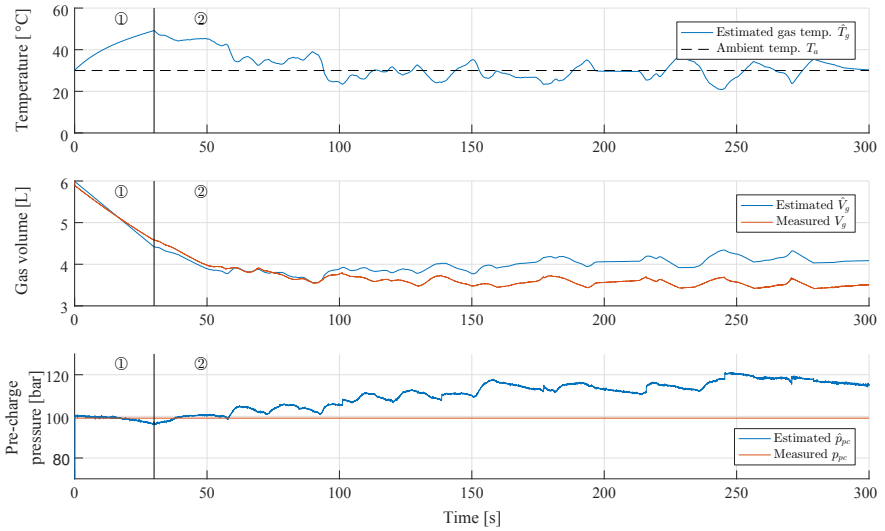

Fig. 4.18: Measured and estimated accumulator states using estimated accumulator flow. Accumulator pre-charge pressure is $p_{pc} = 100$bar. Initial conditions: $\hat{\mathbf{x}}_0 = [\hat{V}_{g0} = 6L \quad \hat{T}_{g0} = 30°C \quad \hat{m}_{g0} = 3 \cdot 10^{-5}kg]$. Figure from paper F.

The estimated gas temperature $\hat{T}_g$ is expectedly seen to fluctuate around the ambient temperature after the initial charging cycle. During region ①, the estimated gas volume $\hat{V}_g$ decreases faster than the measured value. This concurs with described leakage flow in the setup, which is not accounted for in the estimation. $\hat{V}_g$ is seen to slowly drift from the measured value during region ② operation. The gas volume is simply the integral of the accumulator flow, whereby the errors associated with accumulator flow estimation and leakage are causing the drift in estimated gas volume. Consequently, the resulting pre-charge pressure estimate $\hat{p}_{pc}$ is seen to drift during region ②. As discussed in paper F, several parameters could be introduced for

increasing precision of the accumulator flow estimate. Thus, reducing the unacceptable drift in the pre-charge pressure estimate. These parameters are, however, subject to change due to normal wear of the supply system and not investigated further.

In spite of the drifting values, a precise pre-charge pressure estimate is plausible during region ①. Due to low wind speed periods and other production stops, it is not uncommon for a turbine to be started up at least a couple of times a week. Gas leakage may, therefore, be detected before failure as the fault develops over a significantly larger time frame.

A deficiency of using the initial charging cycle for estimation, is the sensitivity to the initial conditions set in the EKF. Fig. 4.19 presents estimation errors based on wrongful setting of the initial conditions, the presence of fluid leakage, and input flow offset. The estimation error is shown for four levels of pre-charge pressure. The pre-charge estimate is determined as the mean value of 5-second data window starting 0.2s after the initial charging cycle is initiated.

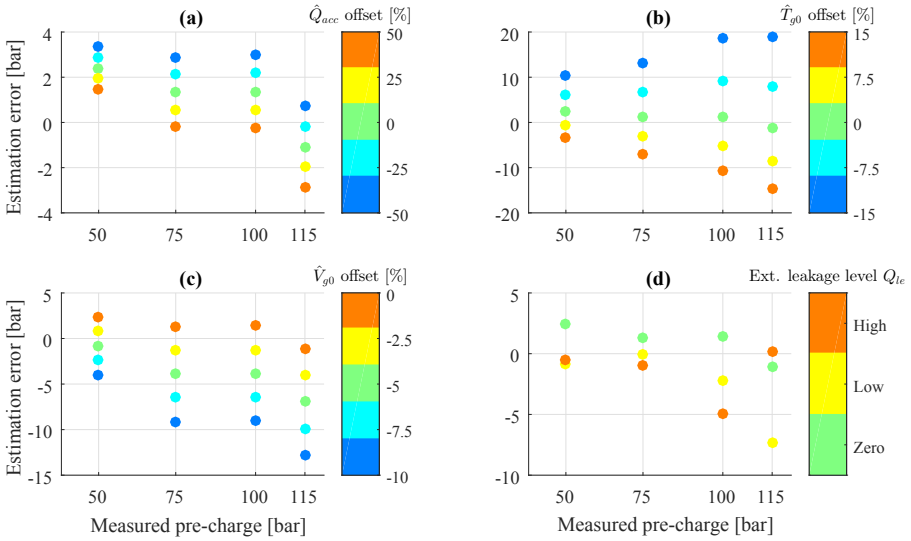

Fig. 4.19: Estimation error of the pre-charge pressure in the case of; **(a)** offset in the input flow, **(b)** offset in the initial condition of the gas temperature, **(c)** offset in the initial condition of the gas volume and **(d)** external leakage. Figure from paper F.

Figure 4.19 (a) shows the estimation error in the event of an offset in the estimated accumulator flow. An estimation error within ±5bar is regarded as highly acceptable even for large offset at ±50%.

In Fig. 4.19 (b) a low robustness is observed towards wrongful setting of the initial gas temperature $\hat{T}_{g0}$. Precise setting of the initial gas temperature is, therefore, necessary for precise estimation of the pre-charge pressure. One

way of ensuring a precise estimate is to utilize the thermal time constant τ_g of the accumulator for determining how long to wait before the gas has settled to the ambient temperature.

The effect of an offset in initial gas volume $\hat{V}_{g0}$ is seen in Fig. 4.19 (c). The estimation error is acceptable for an offset of -5% at pre-charge pressures below 100bar. This highlights the importance of fully draining the accumulator from fluid, before initiating the estimation procedure. Note, that the accumulators can be drained to the reservoir using the valves V6, V7, and V10.

Lastly, estimation in the presence of fluid leakage is evaluated in Fig. 4.19 (d). All estimated values are within an acceptable vicinity of the pre-charge pressure except for low leakage at 115bar pre-charge. It is seen that the estimation error is not necessarily increasing due to increasing external leakage.

As a general remark, the estimation error is seen to reduce at lower pre-charge levels. This is fortunate, as the risk increases at lower levels of pre-charge pressure. The method is, therefore, able to reliably detect gas leakage every time the accumulators are charged from an empty condition. This could be every time the turbine is started up. While promoting detection in a wide range of operating temperatures, the model-based method has not been experimentally validated in other than $T_a = 30°\text{C}$. Previous work [33] has, however, indicated a similar model precision in the range $T_a : \{-20, 60\}°\text{C}$.

Finally, a combination of the previously presented signal-based and the model-based detection procedure allows for gas leakage detection in both accumulator configurations. Detection is permitted during startup and at normal operation above rated wind speed.

5 Closing Remarks

5.1 Conclusions

This thesis considered the improvement of fluid power pitch systems in wind turbines in terms of safety and reliability. The state-of-the-art was established in paper A and improvements were facilitated firstly by analysis of critical failure modes and root causes in papers B and C. Mitigation of critical failure modes and root causes was then handled both for the pitch system design in paper D and through Fault Detection and Diagnosis (FDD) in papers E, F, and G.

As highlighted in the state-of-the-art review in paper A and paper B, only the quantitative modeling of pitch system reliability was previously considered. Hence, the qualitative basis including the fault propagation needed for identification of critical failure modes and root causes were not fully covered. The need for a qualitative approach was additionally emphasized by the lack of detailed field failure data. In paper B, a qualitative framework was presented that described a systematical design tool for performing the qualitative failure analysis of fluid power pitch systems. Verification of the design tool was conducted in a case study of a pitch system where the results showed to comply well with recent field data on failure in pitch systems. Additionally, the results emphasized safety-critical failure modes as internal fluid leakage, valve seizure, and accumulator gas leakage. In regards to reliability, the critical failure modes showed to be external fluid leakage and loss of valve control. The latter either due to seizure or solenoid coil malfunction.

A feasibility study of using a state-of-the-art method for estimating the detailed qualitative failure rates of pitch system components was presented in paper C. The estimation relied on simulated operating conditions. Despite considering a large range of operating conditions and parameter variations, the estimated failure rates were seen to exceed the field data by orders of magnitude. Conclusively, further work is needed to improve the quantitative failure rate estimation techniques for use in fluid power pitch systems.

In connection with the system design, the review presented in paper A revealed closed-type hub-contained fluid power pitch systems to be the dominant alternative to the conventional system suggested in patent and patent

applications. In paper D, a closed-type system was proposed that eliminates high-pressure leakage paths between the hub and the nacelle of the wind turbine. Containment of the system in the rotating hub is facilitated by the use of a bootstrap reservoir. The closed-type concept was compared with the conventional concept by using the design tool. A lowered risk and increased reliability compared to the conventional system were seen for a closed-type concept supplied by a common bootstrap reservoir.

Based on results from the design tool, a significant reduction of the system risk was seen to be obtained when detecting accumulator gas leakage before failure. Paper E dealt with the development and application of a gas leakage detection method utilizing Multiresolution Signal Decomposition (MSD) of the accumulator fluid pressure signal. The method is applicable to accumulators used in normal operation (configuration 1). Simulation results showed the efficacy of the detection for operating conditions for above rated wind speeds, a wide range of turbulence intensities, and ambient temperatures above 22°C. The detection method was rigorously validated on an experimental setup working under similar load conditions as occurring in wind turbines. Experiments additionally showed the detection method to be robust to external fluid leakage. Model-based gas leakage detection using the Extended Kalman Filter (EKF) was proposed in paper F to increase the usable temperature range and applicability to accumulators in configuration 2. Experiments showed that detection failed during normal operation of the turbine due to sensitivity to estimation precision of the input accumulator flow. The results also showed that gas leakage detection was permitted during initial charging of the accumulators. However, special attention should be given to precisely estimate initial conditions for the gas temperature and gas volume. Further work was suggested for combining the signal and model-based method for enabling gas leakage detection in a wider range of conditions.

Coil failure of solenoid valves showed to significantly decrease system reliability. Coil degradation was characterized through extensive accelerated tests which indicated several instances of faults before failure. A method using the EKF for detecting these early signs of coil failure was proposed. Rigorous experiments showed that very reliable and fast detection was obtained over a range of operating conditions. The operating conditions covered an ambient temperature range of 25–45°C, a fluid temperature range of 20–40°C, and free and forced convection.

The overall conclusion was that critical failure modes and root causes, not obvious from available field data, could be identified by the application of the proposed qualitative design tool. Detection methods for fault significant to both safety and reliability have been proposed. If the fault detection methods show similar promising results in actual wind turbine tests as in experiments, great potential lies in their utilization for condition-based maintenance.

5.2 Further Work

Improving the reliability and safety of pitch systems involves multiple interconnected tasks. Both reliability and safety can be addressed in the design of the system's hardware by the choice of concept and components. But also the ability to detect faults before failure and fault mitigation using Fault-Tolerant Control (FTC) influences safety and reliability. The design tool has facilitated the evaluation of these choices in terms of safety and reliability, i.e. risk and failure occurrence respectively. However, further work is needed for determining the actual impact to reliability. Because the available failure rate estimation method is not sufficiently precise, more emphasis should be put on understanding and quantifying failures in fluid power components. Especially important is the investigation and characterization of valve seizure. As shown in this thesis, valve seizure is the most critical failure mode of pitch systems. Characterization of this fault potentially leads to the design of detection methods for alarming on the early signs of failure.

As mentioned, the application of FTC has the potential to increase the availability of pitch systems. While the application of FTC has been investigated for pitch systems, concepts that allow for system reconfiguration could be considered. Extensive research is currently being conducted on the design and application of digital fluid power systems [7, 63, 72, 79, 82, 84]. Such systems employ multiple on/off valves for controlling cylinder motion instead of a single proportional valve. As pointed out in paper D[Fig. 8], the proportional valve is the single most unreliable component of the pitch system and is typically more expensive than simple on/off valves. Reconfiguration in systems employing multiple on/off valves in the event of valve failure may, therefore, pose a cost-effective solution for increasing availability.

An important area, which has not been investigated in this thesis, is the application of the fluid quality for detecting faults in the system. The review presented in paper A points to several early studies, that indicate the use of the fluid condition for detecting component degradation. While this is already done for the gearbox lubricant in wind turbines, further work is needed for adaption to the fluid power pitch system [31].

References

[1] S. Angadi, R. Jackson, S. yul Choe, G. Flowers, J. Suhling, Y.-K. Chang, J.-K. Ham, and J. il Bae, "Reliability and life study of hydraulic solenoid valve. part 2: Experimental study," *Engineering Failure Analysis*, vol. 16, no. 3, pp. 944–963, 2009.

[2] H. Arabian-Hoseynabadi, H. Oraee, and P. Tavner, "Failure Modes and Effects Analysis (FMEA) for wind turbines," *International Journal of Electrical Power & Energy Systems*, vol. 32, no. 7, pp. 817–824, 2010.

[3] R. Atkinson, M. Montakhab, K. Pillay, D. Woollons, P. Hogan, C. Burrows, and K. Edge, "Automated fault analysis for hydraulic systems: Part 1: Fundamentals," *Proceedings of the Institution of Mechanical Engineers, Part I: Journal of Systems and Control Engineering*, vol. 206, no. 4, pp. 207–214, 1992.

[4] V. P. Bacanskas, G. C. Roberts, and G. J. Toman, "Aging and service wear of solenoid-operated valves used in safety systems of nuclear power plants: Volume 1, Operating experience and failure identification," Oak Ridge National Laboratory, Tech. Rep. ORNL/Sub/83-28915/4/V1, 1987.

[5] G. A. Barnard, "Control charts and stochastic processes," *Journal of the Royal Statistical Society. Series B (Methodological)*, vol. 21, no. 2, pp. 239–271, 1959.

[6] R. Bauer, C. Weisser, I. Bork, S. Weiss, B. Zickgraf, and S. Spindler, "Method for determining a position of a piston in a piston pressure accumulator by means of inductive sensors and suitably designed piston pressure accumulator," US Patent 20 140 360 360, Dec. 11, 2014, uS Patent App. 14/370,024.

[7] N. C. Bender, H. C. Pedersen, A. Plöckinger, and B. Winkler, "Towards a modelling framework for designing active check valves - a review of state-of-the-art," *International Journal of Fluid Power*, 2017.

[8] B. Bertsche, *Reliability in automotive and mechanical engineering: determination of component and system reliability*. Springer Science & Business Media, 2008.

[9] A. Birolini, *Reliability Engineering Theory and Practice*, 7th ed. Springer-Verlag Berlin Heidelberg, 2014.

[10] M. Blanke and J. Schröder, *Diagnosis and fault-tolerant control*. Springer, 2006, vol. 691.

[11] M. Börner, H. Straky, T. Weispfenning, and R. Isermann, "Model based fault detection of vehicle suspension and hydraulic brake systems," *Mechatronics*, vol. 12, no. 8, pp. 999–1010, 2002.

[12] D. R. Bull, C. R. Burrows, W. J. Crowther, K. A. Edge, R. M. Atkinson, P. G. Hawkins, D. J. Woollons *et al.*, "Approaches to automated FMEA of hydraulic systems," *Procceddings of the ImechE Congress Aerotech Seminar, Birmingham*, 1995.

[13] D. R. Bull, J. S. Stecki, K. A. Edge, and C. R. Burrows, "Failure modes and effects analysis of a valve-controlled hydrostatic drive," *Challenges and Solutions: Tenth Bath International Fluid Power Workshop*, pp. 131–144, 1997.

[14] C. S. Burrus, R. A. Gopinath, and H. Guo, *Introduction to wavelets and wavelet transforms: A Primer*, 1st ed. IBC Plaza Houston, Houston, Texas: OpenStax, 1998.

[15] J. Carroll, A. McDonald, and D. McMillan, "Failure rate, repair time and unscheduled O&M cost analysis of offshore wind turbines," *Wind Energy*, pp. 1107–1119, 2015.

[16] L. Chen, F. Shi, and R. Patton, "Active ftc for hydraulic pitch system for an offshore wind turbine," *Conference on Control and Fault-Tolerant Systems (SysTol)*, pp. 510–515, 2013.

[17] M. Choux, I. Tyapin, and G. Hovland, "Leakage-detection in blade pitch control systems for wind turbines," *Reliability and Maintainability Symposium (RAMS), 2012 Proceedings-Annual*, pp. 1–7, 2012.

[18] I. Dülk and T. Kovácsházy, "Sensorless position estimation in solenoid actuators with load compensation," *IEEE International Instrumentation and Measurement Technology Conference Proceedings*, pp. 268–273, May 2012.

[19] P. Dvorak, "Hydraulic pitch control for wind-turbine blades," Windpower Engineering, May 16 2009, retrieved 07-01-2016. [Online]. Available: http://www.windpowerengineering.com/design/mechanical/gearboxes/hydraulic-pitch-control-for-wind-turbine-blades/

[20] N. Fichaux, J. Beurskens, P. H. Jensen, and J. Wilkes, "Upwind: Design limits and solutions for very large wind turbines," EWEA, Tech. Rep. 019945 (SES6), Mar. 2011.

[21] Y. Gao, Q. Zhang, and X. Kong, "Wavelet based pressure analysis for hydraulic pump health diagnosis," *Transactions of the ASAE*, vol. 46, no. 4, pp. 969–976, 2003.

[22] V. Gjerstad, T. Lauvas, and M. Grahl Madsen, "FMECA of an offshore man-riding winch," *Proceedings of Power Transmission and Motion Control*, pp. 183–197, 2003.

[23] GL, *Guideline for the Certification of Offshore Wind Turbines*, 2012th ed., GL, Germanischer Lloyd Industrial Services GmbH Renewables Certification Brooktorkai 18, 20457 Hamburg, Germany, 2012.

[24] Global Wind Energy Council & Institute for Sustainable Futures, "Global wind energy outlook 2016," *GWEC*, vol. 6., Oct. 2016.

[25] A. Y. Goharrizi, "Leakage fault detection in hydraulic actuators based on wavelet transform," Ph.D. dissertation, University of Manitoba, Dec. 2010.

[26] A. Y. Goharrizi and N. Sepehri, "A wavelet-based approach to internal seal damage diagnosis in hydraulic actuators," *IEEE Transactions on Industrial Electronics*, vol. 57, no. 5, pp. 1755–1763, 2010.

[27] ——, "A wavelet-based approach for external leakage detection and isolation from internal leakage in valve-controlled hydraulic actuators," *IEEE Transactions on Industrial Electronics*, vol. 58, no. 9, pp. 4374–4384, 2011.

[28] ——, "Application of fast fourier and wavelet transforms towards actuator leakage diagnosis: A comparative study," *International Journal of Fluid Power*, vol. 14, no. 2, pp. 39–51, 2013.

[29] J. C. Goldfrank and H. W. Cooper, "Benedict-Webb-Rubin constants and new correlations," *Hydrocarbon Processing*, vol. 46, no. 12, 1967.

[30] J. Gratzmuller, "Piston-type hydropneumatic accumulator equipped with a gas shortage detection device," US Patent 4,243,856, Jan. 6, 1981.

[31] Z. Hameed, J. Vatn, and J. Heggset, "Challenges in the reliability and maintainability data collection for offshore wind turbines," *Renewable Energy*, vol. 36, no. 8, pp. 2154–2165, 2011.

[32] X. Han, H. Zhang, Y. Chen, X. Zhang, and C. Wang, "Fault diagnosis of hydraulic variable pitch for wind turbine based on qualitative and quantitative analysis," *World Congress on Intelligent Control and Automation (WCICA), 2012 10th*, pp. 3181–3185, 2012.

[33] H. B. Hansen and P. W. Rasmussen, "Modeling hydraulic accumulators for use in wind turbines," *13th Scandinavian International Conference on Fluid Power*, no. 092, pp. 327–334, June 2013.

[34] M. O. Hansen, *Aerodynamics of wind turbines*, 2nd ed. earthscan London, 2008.

[35] S. Haykin, *Kalman filtering and neural networks*. Wiley Online Library, 2001.

[36] N. Helwig, E. Pignanelli, and A. Schütze, "Condition monitoring of a complex hydraulic system using multivariate statistics," *IEEE International Instrumentation and Measurement Technology Conference (I2MTC) Proceedings*, pp. 210–215, May 2015.

[37] V. A. Hines, A. B. Ogilvie, and C. R. Bond, "Continuous reliability enhancement for wind (crew) database: Wind plant reliability benchmark," Sandia National Laboratories, Tech. Rep., Sep. 2013.

[38] P. A. Hogan, C. R. Burrows, K. A. Edge, R. M. Atkinson, M. R. Montakhab, and D. J. Woollons, "Automated fault analysis for hydraulic systems: Part 2: Applications," *Proceedings of the Institution of Mechanical Engineers, Part I: Journal of Systems and Control Engineering*, vol. 206, no. 4, pp. 215–224, 1992.

[39] ——, "Automated fault tree analysis for hydraulic systems," *Journal of Dynamic Systems, Measurement, and Control*, vol. 118, no. 2, pp. 278–282, Jun. 1996.

[40] J. L. Holst and A. Pedersen, "Increasing the owners' value of wind power plants in energy systems with large shares of wind energy," *Danish Wind Industry Association, Megavind*, Oct. 2014.

[41] T. Hosoda, N. Nakanishi, H. Shibata, and T. Saito, "Device for detecting leakage of precharged gas from gas-type accumulator," US Patent 4,870,390, Sep. 26, 1989, 4,870,390.

[42] T. M. Hunt, *Handbook of wear debris analysis and particle detection in liquids*. Netherlands: Springer Science & Business Media, 1993.

[43] IEC, "Wind turbines part 1: Design requirements (IEC 61400-1:2005)," International Electrotechnical Commission, 2006.

[44] N. J. Jameson, M. H. Azarian, and M. Pecht, "Impedance-based condition monitoring for insulation systems used in low-voltage electromagnetic coils," *IEEE Transactions on Industrial Electronics*, vol. 64, no. 5, pp. 3748–3757, 2017.

[45] ——, "Fault diagnostic opportunities for solenoid operated valves using physics-of-failure analysis," *International Conference on Prognostics and Health Management*, 2014.

[46] ——, "Thermal degradation of polyimide insulation and its effect on electromagnetic coil impedance," *Proceedings of the Society for Machinery Failure Prevention Technology Conference*, 2017.

[47] T. L. Jones, *Handbook of Reliability Prediction Procedures for Mechanical Equipment*. West Bethesda, Maryland 20817-5700: Naval Surface Warfare Center NSWC, May 2011.

[48] J. Jonkman, "TurbSim user's guide: Version 1.50," National Renewable Energy Laboratory, 1617 Cole Boulevard, Golden, Colorado 80401-3393, Technical Report NREL/TP-500-46198, August 2009.

[49] J. Jonkman and M. L. J. Buhl, "FAST user's guide," National Renewable Energy Laboratory, 1617 Cole Boulevard, Golden, Colorado 80401-3393, Technical Report NREL/EL-500-29798, August 2005.

[50] J. Jonkman, S. Butterfield, W. Musial, and G. Scott, "Definition of a 5-MW reference wind turbine for offshore system development," National Renewable Energy Laboratory, 1617 Cole Boulevard, Golden, Colorado 80401-3393, Technical Report NREL/TP-500-38060, February 2009.

[51] V. Jouppila, J. Kuusisto, and A. Ellman, "A model-based method for condition monitoring of a proportional valve," *Proceedings of the Bath Workshop on Power Transmission and Motion Control, PTMC*, pp. 309–317, 2004.

[52] M. Khoshzaban-Zavarehi, "On-line condition monitoring and fault diagnosis in hydraulic system components using parameter estimation and pattern classification," Ph.D. dissertation, University of British Columbia, 1997.

[53] W. Kruckewitt and H. Plettner, "High pressure accumulator," US Patent 4,611,634, Sep. 16, 1986, 4,611,634.

[54] R. C. Kryter, "Aging and service wear of solenoid-operated valves used in safety systems of nuclear power plants: Volume 2, Evaluation of Monitoring Methods," Oak Ridge National Laboratory, Tech. Rep. ORNL/Sub/83-28915/4/V1, 1992.

[55] P. Lako and M. Koyama, "Wind power: Technology brief," IEA-ETSAP and IRENA, Masdar City, PO Box 236, Abu Dhabi, United Arab Emirates, Tech. Rep., Mar. 2016.

[56] J. Liniger, H. C. Pedersen, and M. Soltani, "Reliable fluid power pitch systems: A review of state of the art for design and reliability evaluation of fluid power systems," *Proceedings of the ASME/BATH 2015 Symposium on Fluid Power & Motion Control*, pp. 1–10, October 2015.

[57] ——, "Model-based estimation of gas leakage for fluid power accumulators in wind turbines," *Proceedings of the ASME/BATH 2017 Symposium on Fluid Power & Motion Control*, pp. 1–10, October 2017.

[58] ——, "Risk-based comparative study of fluid power pitch concepts," *Proceedings of the ASME/BATH 2017 Symposium on Fluid Power & Motion Control*, pp. 1–9, October 2017.

[59] J. Liniger, H. C. Pedersen, M. N. Soltani, and N. Sepehri, "Feasibility study of a simulation driven approach for estimating reliability of wind turbine fluid power pitch systems," *Submitted to: Proceedings of European Safety and RELiability Conference (ESREL)*, 2018.

[60] J. Liniger, N. Sepehri, M. Soltani, and H. C. Pedersen, "Signal-based gas leakage detection for fluid power accumulators in wind turbines," *Energies*, vol. 10, no. 3, pp. 1–18, Mar. 2017.

[61] J. Liniger, M. Soltani, H. C. Pedersen, J. Carroll, and N. Sepehri, "Reliability based design of fluid power pitch systems for wind turbines," *Wind Energy*, vol. 20, no. 6, pp. 1097–1110, June 2017.

[62] J. Liniger, S. Stubkier, H. C. Pedersen, and M. Soltani, "Early detection of coil failure in solenoid valves," *Submitted to: IEEE/ASME Transactions on Mechatronics*, 2018.

[63] M. Linjama, M. Paloniitty, L. Tiainen, and K. Huhtala, "Mechatronic design of digital hydraulic micro valve package," *Procedia Engineering*, vol. 106, pp. 97–107, 2015.

[64] S. G. Mallat, "A theory for multiresolution signal decomposition: the wavelet representation," *IEEE transactions on pattern analysis and machine intelligence*, vol. 11, no. 7, pp. 674–693, 1989.

[65] G. Mauri, "Integrating safety analysis techniques, supporting identification of common cause failures," Ph.D. dissertation, Department of Computer Science, The University of York, Sep. 2000.

[66] P. Mbari and D. McCandlish, "Reliability and fault tree analysis in hydraulic systems," *Proceedings of the 7th International Fluid Power Symposium*, pp. 303–311, Sep. 1986.

[67] J. R. Mercer, "Reliability of solenoid valves," *Proceedings of the Institution of Mechanical Engineers*, vol. 184, no. 2, pp. 89–94, 1969.

[68] H. E. Merritt, *Hydraulic control systems*. John Wiley & Sons, 1967.

[69] T. Minami, Y. Yatomi, and H. Doi, "Wind turbine generator and soundness diagnosis method thereof," US Patent Application 12/675,258, Dec. 15, 2011, 12/675,258.

[70] S. Nielsen, J. Nielsen, and J. B. Nielsen, "Wind turbine blade pitch system," EU Patent Application 20,110,172,065, Jan. 4, 2012, 20,110,172,065.

[71] NordzeeWind, "Operations report 2009," NordzeeWind, Tech. Rep. OWEZ_R_000_20101112, November 2010.

[72] C. Nørgaard, "Design, optimization and testing of valves for digital displacement machines," Ph.D. dissertation, 2017.

[73] P. F. Odgaard, J. Stoustrup, and M. Kinnaert, "Fault tolerant control of wind turbines: a benchmark model," *Elsevier IFAC Publications / IFAC Proceedings series*, 2009.

[74] D. Otis and A. Pourmovahed, "An algorithm for computing nonflow gas processes in gas springs and hydropneumatic accumulators," *Journal of dynamic systems, measurement, and control*, vol. 107, no. 1, pp. 93–96, 1985.

[75] D. Parquet, "Accumulator warning system," US Patent 4,014,213, Mar. 29, 1977, 4,014,213.

[76] H. C. Pedersen, T. O. Andersen, and J. Liniger, "Investigation of load reduction possibilities in wind turbines using a fluid power pitch system," in *Proceedings of the ASME/BATH 2015 Symposium on Fluid Power & Motion Control*. American Society of Mechanical Engineers, October 2015.

[77] J. Perotti, A. Lucena, and B. Burns, "Smart actuators: Valve Health Monitor (vhm) system," *Proceedings of Defence and Security Symposium, Sensors for Propulsion Measurement Applications*, vol. 6222, pp. 6222 – 6222 – 10, 2006.

[78] A. Pfeffer, T. Glück, W. Kemmetmüller, and A. Kugi, "State of charge estimator design for a gas charged hydraulic accumulator," *Journal of Dynamic Systems, Measurement and Control*, vol. 137, no. 6, 2015.

[79] A. Ploeckinger, B. Winkler, and R. Scheidl, "Development and prototyping of a compact, fast 3/2 way switching valve with integrated onboard electronics," in *Proceedings of the 11th Scandinavian International Conference on Fluid Power*. Linköping Sweden, 2009.

[80] A. Pourmovahed and D. Otis, "An experimental thermal time-constant correlation for hydraulic accumulators," *Journal of dynamic systems, measurement, and control*, vol. 112, no. 1, pp. 116–121, 1990.

[81] J. Ribrant and L. Bertling, "Survey of failures in wind power systems with focus on swedish wind power plants during 1997-2005," *IEEE Transactions on Energy Conversion*, vol. 22, no. 1, pp. 1–8, March 2007.

[82] D. Roemer, "Design and optimization of fast switching valves for large scale digital hydraulic motors," Ph.D. dissertation, 2014.

[83] S. Rotthäuser, "Verfahren zur berechnung und untersuchung hydropneumatischer speicher," PhD thesis, Fakultät für Maschinenwesen der Rheinisch-Westfälischen Technischen Hochschule Aachen, Essen, Germany, 1993.

[84] N. Sell, D. Johnston, A. Plummer, and S. Kudzma, "Development of a position controlled digital hydraulic valve," *Proceedings of the ASME/BATH 2015 Symposium on Fluid Power and Motion Control*, 10 2015.

[85] F. Shi and R. J. Patton, "A robust adaptive approach to wind turbine pitch actuator component fault estimation," *Conference on Control (CONTROL), 2014 UKACC International*, pp. 468–473, 2014.

[86] R. F. Stapelberg, *Handbook of reliability, availability, maintainability and safety in engineering design*. London: Springer Science & Business Media, 2009.

[87] J. S. Stecki, F. Conrad, and B. Oh, "Software tool for automated failure modes and effects analysis (FMEA) of hydraulic systems," *Proceedings of the JFPS International Symposium on Fluid Power*, no. 5-3, pp. 889–894, 2002.

[88] P. Tavner, *Offshore wind turbines: reliability, availability and maintenance*, ser. Renewable Energy Series. Institution of Engineering and Technology, 2012, vol. 13.

[89] P. J. Tavner, A. Higgins, H. Arabian, H. Long, and Y. Feng, "Using an FMEA method to compare prospective wind turbine design reliabilities," vol. 4, pp. 2501–2537, 2010.

[90] G. E. Totten, *Handbook of hydraulic fluid technology*. Boca Raton, Florida: CRC Press, 2011.

[91] US Department of Defence, *MIL-STD-1629A: Procedures for Performing A Failure Mode, Effects and Criticality Analysis*, US Military Standard MIL-STD-1629A, November 1980.

[92] J. Watton, *Modelling, monitoring and diagnostic techniques for fluid power systems*. London: Springer Science & Business Media, 2007.

[93] M. Wilkinson and B. Hendriks, "Reliability-focused research on optimizing wind energy system design, operation and maintenance: Tools, proof of concepts, guidelines & methodologies for a new generation," *Collaborative Project: Large Scale Integrated Project, FP7-ENERGY-2007-1-RTD*, 2010.

[94] X. Wu, Y. Li, F. Li, Z. Yang, and W. Teng, "Adaptive estimation-based leakage detection for a wind turbine hydraulic pitching system," *Mechatronics, IEEE/ASME Transactions on*, vol. 17, no. 5, pp. 907–914, 2012.

[95] X. Yang, J. Li, W. Liu, and P. Guo, "Petri net model and reliability evaluation for wind turbine hydraulic variable pitch systems," *Energies*, vol. 4, no. 6, pp. 978–997, 2011.

[96] A. Yuge, T. Hayashi, and M. Yamada, "Wind turbine generator and valve function checking method for wind turbine generator," Patent, Dec. 5, 2013, US Patent App. 13/484,373.

Part II

Contributions

Paper A

Reliable Fluid Power Pitch Systems: A Review of State of the Art for Design and Reliability Evaluation of Fluid Power Systems

Jesper Liniger, Henrik C. Pedersen and Mohsen Soltani

The paper has been published in the
Proceedings of the ASME/BATH 2015 Symposium on Fluid Power & Motion Control, ASME Digital Collection, 2015

The layout has been revised, and small editorial changes have been made. Content relevant changes, if any, are marked with explicit footnotes.

Paper B

Reliability Based Design of Fluid Power Pitch Systems for Wind Turbines

Jesper Liniger, Mohsen Soltani, Henrik C. Pedersen, James Carroll and Nariman Sepehri

The paper has been published in
Wind Energy, vol. 20, pp. 1097-1110

Paper C

Feasibility Study of a Simulation Driven Approach for Estimating Reliability of Wind Turbine Fluid Power Pitch Systems

Jesper Liniger, Henrik C. Pedersen, Mohsen Soltani and Nariman Sepehri

Abstract accepted and under review for the
European Safety and Reliability Conference 2018, European Safety and Reliability Association

The layout has been revised, and small editorial changes have been made. Content relevant changes, if any, are marked with explicit footnotes.

Paper D

Risk-based Comparative Study of Fluid Power Pitch Concepts

Jesper Liniger, Henrik C. Pedersen and Mohsen Soltani

The paper was nominated for "Best Paper" by the Global Fluid Power Society.

The paper has been published in the
Proceedings of the ASME/BATH 2017 Symposium on Fluid Power & Motion Control, ASME Digital Collection, 2017

Paper E

Signal-based Gas Leakage Detection for Fluid Power Accumulators in Wind Turbines

Jesper Liniger, Nariman Sepehri, Mohsen Soltani and Henrik C. Pedersen

The paper has been published in
Energies, Multidisciplinary Digital Publishing Institute, 2017, vol. 10

Paper F

Model-based Estimation of Gas Leakage for Fluid Power Accumulators in Wind Turbines

Jesper Liniger, Henrik C. Pedersen and Mohsen Soltani

The paper has been published in the
Proceedings of the ASME/BATH 2017 Symposium on Fluid Power & Motion Control, ASME Digital Collection, 2017

Paper G

Early Detection of Coil Failure in Solenoid Valves

Jesper Liniger, Henrik C. Pedersen, Mohsen Soltani and Søren Stubkier

The paper is submitted to
IEEE/ASME Transactions on Mechatronics, 2018

ISSN (online): 2446-1636
ISBN (online): 978-87-7210-144-6

AALBORG UNIVERSITY PRESS